Journal of Molecular Structure 1272 (2023) 134154

Contents lists available at ScienceDirect

Journal of Molecular Structure

journal homepage: www.elsevier.com/locate/molstr

Synthesis, *in vitro* and *in silico* studies on novel 3-aryloxymethyl-5-[(2-oxo-2-arylethyl)sulfanyl]-1,2,4-triazoles and their oxime derivatives as potent inhibitors of mPGES-1

Gizem Erensoy[a,1], Kai Ding[b,c], Chang-Guo Zhan[b,c], Gamze Çiftçi[d], Kemal Yelekçi[d], Merve Duracık[e], Özlem Bingöl Özakpınar[e], Esra Aydemir[f,g], Zübeyde Nur Yılmaz[f], Fikrettin Şahin[f], Necla Kulabaş[h], Esra Tatar[h], İlkay Küçükgüzel[h,*]

[a] Department of Pharmaceutical Chemistry, Institute of Health Sciences, Marmara University, Kartal 34865, İstanbul, Turkey
[b] Department of Pharmaceutical Sciences, College of Pharmacy, University of Kentucky, 789 South Limestone Street, Lexington, KY 40536, United States
[c] Center for Pharmaceutical Research and Innovation, College of Pharmacy, University of Kentucky, 789 South Limestone Street, Lexington, KY 40536, United States
[d] Department of Bioinformatics and Genetics, Faculty of Engineering and Natural Sciences, Kadir Has University, 34083, İstanbul, Turkey
[e] Department of Biochemistry, Faculty of Pharmacy, Marmara University, Maltepe 34854, İstanbul, Turkey
[f] Department of Genetics and Bioengineering, Faculty of Engineering, Yeditepe University, Kayışdağı, İstanbul, Turkey
[g] Department of Biomedical Engineering, Faculty of Engineering and Natural Sciences, Biruni University, Zeytinburnu, 34010, İstanbul, Turkey
[h] Department of Pharmaceutical Chemistry, Faculty of Pharmacy, Marmara University, Maltepe 34854, İstanbul, Turkey

ARTICLE INFO

Article history:
Received 20 June 2022
Revised 8 September 2022
Accepted 13 September 2022
Available online 14 September 2022

Key words:
mPGES-1
Inflammation
Cancer
Angiogenesis
1,2,4-triazoles
Molecular docking

ABSTRACT

Human microsomal prostaglandin E synthase (mPGES)-1 is a glutathione-dependent membrane-bound enzyme which is involved in the terminal stage of prostaglandin E2 (PGE_2) synthesis. It has been well reported as a key target for the discovery of new anti-inflammatory and anti-cancer drugs. Specific inhibitors of mPGES-1 are anticipated to selectively restrain the generation of PGE_2 induced by the inflammatory stimuli, without obstructing of the regular biosynthesis of other homeostatic prostanoids. Therefore, the design of mPGES-1 inhibitors can represent a better choice to take control of PGE_2 associated diseases, compared with conventional non-steroidal anti-inflammatory drugs and cyclooxygenase (COX) inhibitors, which are known for their serious side effects. Although there is an intensive effort for the identification of mPGES-1 inhibitors, none of the unveiled molecules so far have reached the clinical market. Therefore, the development of novel mPGES-1 inhibitors with proper drug-like properties is still an unmet medical need. As a continuation of our research for the identification of new chemotypes which might inhibit this enzyme, we now report the design and synthesis of 3-aryloxymethyl-5-[(2-oxo-2-arylethyl)sulfanyl]-1,2,4-triazoles and their oxime derivatives as inhibitors of human mPGES-1. All synthesized compounds were characterized by FTIR, ^{1}H NMR, ^{13}C NMR (for compounds **12, 14, 15, 26, 27**), HMBC (for compounds **6, 7, 8, 16, 19, 23, 28),** and MS data. Twenty-four target compounds **7–30** were screened for their mPGES-1/COX-2 inhibitory activities as well as their cytotoxicity. Of these compounds, **20** and **24** showed potent mPGES-1 inhibition by IC_{50} values of 0.224±0.070 μM and 1.08±0.35 μM, respectively. These two compounds have also been observed to inhibit angiogenesis in matrigel tube formation assay with no toxicity toward HUVEC cells. *In silico* studies were also held to understand inhibition mechanisms of the most active compounds using molecular docking, molecular dynamics calculations and ADMET predictions.

1. Introduction

Prostaglandins (PGs) and leukotrienes are important bio-active derivatives of arachidonic acid which have essential roles in physiological events in the human body such as homeostasis, fever, gastrointestinal motility, pain, and inflammation [1]. Cyclooxygenases (COX-1 and COX-2) are the key enzymes to produce PGH_2 from arachidonic acid. Several structurally related PGs including PGE_2, PGD_2, $PGF_{2\alpha}$ and PGI_2 are synthesized from PGH_2 with respective enzymes.

* Corresponding author.
E-mail address: ikucukguzel@marmara.edu.tr (İ. Küçükgüzel).
[1] Present address: Department of Biology and Biological Engineering, Chalmers University of Technology, Gothenburg, Sweden.

https://doi.org/10.1016/j.molstruc.2022.134154
0022-2860/

PGE_2 is the most abundant PG among them and has four types of E prostanoid receptors (EP)1–4 [2]. PGE_2 is responsible for vascular inflammation when it is expressed in large amounts. It is known that this process is carried out competitively by prostaglandin I synthase and microsomal prostaglandin E synthase (mPGES)−1 enzyme [3]. The isomerization from PGH_2 to PGE_2 is catalyzed with three different PGE synthases: mPGES-1, mPGES-2 and cPGES (cytosolic). In 1999, mPGES-1 was first characterized [4] and found responsible for various biological events including hemostasis [5]. Normally, mPGES-1 is expressed in low amounts but is easily induced by endotoxins such as interleukin 1β, lipopolysaccharides and epidermal growth factor in pre-inflammatory conditions [6]. COX-1 and mPGES-2 are responsible for the synthesis of the normal amount of PGE_2, whereas COX-2 and mPGES-1 enzymes are responsible for the excessive production of PGE_2. The relationship between COX-2 and mPGES-1 was also converted to a measurement unit and found that the distinction between the active sites of COX-2 and mPGES-1 enzymes is less than 14.4 Å. In inflammation, COX-2 and mPGES-1 are responsible for the production of pathogenic amounts of PGE_2 [3]. mPGES-1 is an attractive target for many diseases such as Alzheimer's disease, atherosclerosis, rheumatoid arthritis, and infant apnea, [7] and studies have been going on for the development of novel mPGES-1 inhibitors. However, none of these candidates has reached clinical trials except phase I studies [8,9] because of the differences between species [10]. Three amino acids located on the active site of human and rodent enzymes are not compatible [11]. These differences in human and mouse mPGES-1 enzymes explain the reason that the two compounds known as MF63 [2-(6–chloro-1*H*-phenanthro-[9,10-d]imidazol-2-yl)isophthalonitrile] and PF-9184 [N-(3′,4′-dichloro[1,1′-biphenyl]−4-yl)−4–hydroxy-2H-1,2-benzothiazine-3-carboxamide 1,1-dioxide] inhibit the human mPGES-1 whereas they do not inhibit the rodent enzyme [7,10]. To overcome this problem, many different mPGES-1 inhibition models being used, such as gene deletion [12–14] and the usage of human xenografts on rodents [15,16]. Cell free assays are also used for the determination of IC_{50} values tPGES-1. MK-886 [1-[(4-chlorophenyl)methyl]−3-[(1,1-dimethylethyl)thio]-α,α-dimethyl-5-(1-methylethyl)−1H-indole-2-propanoic acid] inhibits mPGES-1 *in vitro* in the nanomolar range, whereas no inhibitory effect has been detected in human whole blood assay due to strong protein binding and poor cell permeability [17]. mPGES-1 enzyme has been reported to be associated with many types of cancer, such as; colon [14], lung [18], breast [12], prostate [19], gastric adenocarcinoma [20], and neuroblastoma [21]. Since it is known that COX-2 enzyme can also be present in cancer cells, these two enzymes have gained importance as new targets in cancer treatment [19]. It is also well known that mPGES-1 is related to the induction of tumor progression [4,20,22–25]. Genetic deletion of mPGES-1 reduces proliferation and angiogenesis [15]. MK-886, a well-known mPGES-1 inhibitor, was also found to induce apoptosis by activating caspase-3 [26].

In addition, PGs also play an important role in angiogenesis. PGE_2, which can act on cancer cells, stimulates angiogenic behavior by prompting them to produce proangiogenic factors such as VEGF, basic fibroblast growth factor (bFGF), and the chemokine CXCL1 cells [27–30]. Recent studies have shown that the stromal PGE_2-EP3 receptor is essential for tumor growth and angiogenesis [31]. Studies revealed that tumor-induced angiogenesis was reduced as well as inhibition of chronic inflammation in mPGES-1 enzyme knocked-out mice [32–34].

Triazoles are biologically active heterocyclic compounds and show a wide variety of different biological effects including antiviral [35,36], antituberculosis [37–39], anti-inflammatory [40–43], anticancer [44–47] anti-urease [48], antifungal [49–51], and antiparasitic [52,53] effects. In a study of virtual screening of novel mPGES-1 inhibitors, the compound containing 1,2,4-triazole and thioether structure showed an inhibitory effect at 9.3 nM in cell free assay. However, in human whole blood assay, inhibitory concentration of this molecule has been found 0.7 µM [54]. In our recent work, we also reported the first thioether-oxadiazole hybrid as an mPGES-1 inhibitor [55] (Fig. 1).

Based on these knowledge regarding mPGES-1 and COX enzymes as possible targets, we designed and synthesized 1,2,4-triazole-3-thiones and their thioether derivatives containing ketone and oxime groups. We wish to report for first time both mPGES-1 inhibition and anti-angiogenesis effect of triazole-thioether conjugates containing ketone and oxime functions.

2. Material and methods

2.1. Chemistry

All solvents and reagents were obtained from commercial sources and used without further purification. The purity of the compounds was confirmed by thin-layer chromatography (TLC) performed on Merck silica gel 60 F254 aluminum sheets (Merck, Darmstadt, Germany), using developing systems either S1: chloroform/methanol/acetic acid (8:2:400 µL v/v/v) or S2: petroleum ether/ethyl acetate (5:5 v/v) or S3: petroleum ether/ethyl acetate (7:3 v/v). Spots were detected under UV light at 254 nm. All melting points were determined using Thermo Scientific IA9300 basic model point apparatus and are uncorrected. Elemental analyses were obtained by using Leco CHNS-932 and were consistent with the assigned structures. Infrared spectra were recorded on Shimadzu FT-IR 8400 s and data are expressed in wavenumber (cm^{-1}). ^1H and ^{13}C NMR spectra were recorded on Brüker AVANCE DPX 300 or 600 MHz for ^1H NMR and 150 MHz or 75 MHz for ^{13}C NMR in DMSO–d_6 using tetramethylsilane as the internal standard. All chemical shifts were recorded as δ (ppm). All coupling constants are reported as Hertz. The high-pressure liquid chromatographic system consists of a Shimadzu LC-20AT series instrument equipped with quaternary solvent delivery system and a model SPD-M20A PDA detector. A Rheodyne syringe loading injector with 50 µL sample loop was used for the injection of the compounds. Chromatographic data were collected and processed using Shimadzu LabSolutions software. The separation was performed at ambient temperature by using reversed phase GL Sciences Inertsil ODS-3 (46 × 260 mm, 5 µm) column. All experiments were performed in isocratic mode. The mobile phase was prepared by mixing acetonitrile and water (70:30, v/v) and filtered through a 0.45 µm pore filter, and subsequently degassed by ultrasonication, before use. Solvent delivery was employed at a flow rate of 1 mL/min. Detection of the compounds was carried out at 254 nm.

2.1.1. Synthesis of compound 1

Carvacrol (0.06 mol) and anhydrous potassium carbonate (0.09 mol) were dissolved in dry acetone and refluxed for 4 h. After dropwise addition of ethyl bromoacetate (0.063 mol) within 1 h, the solution was stirred for further 8 h. The solvent was evaporated, then crushed ice was added to the reaction medium. The mixture was stirred for half an hour and extracted with diethyl ether afterward. The organic layer was dried with anhydrous Na_2SO_4, then evaporated under vacuum to leave a yellowish oil. The compound was used without further purification [56]. HPLC t_R (min): 13.92, TLC R_f: 0.74 (S1) yield 80%. IR ν: 1760 (C=O), 1197 (C–O–C). ^1H NMR (300 MHz, DMSO–d_6): δ 1.16 (d, 6H, $J = 6.9\,Hz$, -CH(C**H**$_3$)$_2$); 1.21 (t, 3H, $J = 7.2$ Hz, -CH_2–C**H**$_3$), 2.14 (s, 3H, Ar-C**H**$_3$); 2.80 (septet, 1H, $J = 6.9\,Hz$, -**CH**$(CH_3)_2$); 4.17 (q, 2H, $J = 7.2$ Hz, -C**H**$_2$–CH_3); 4.78 (s, 2H, –S–CH_2–); 6.68 (s, 1H, Ar-**H**), 6.73 (d, 1H, $J = 7.8\,Hz$, Ar–**H**); 7.04 (d, 1H, $J = 7.8\,Hz$, Ar-**H**).

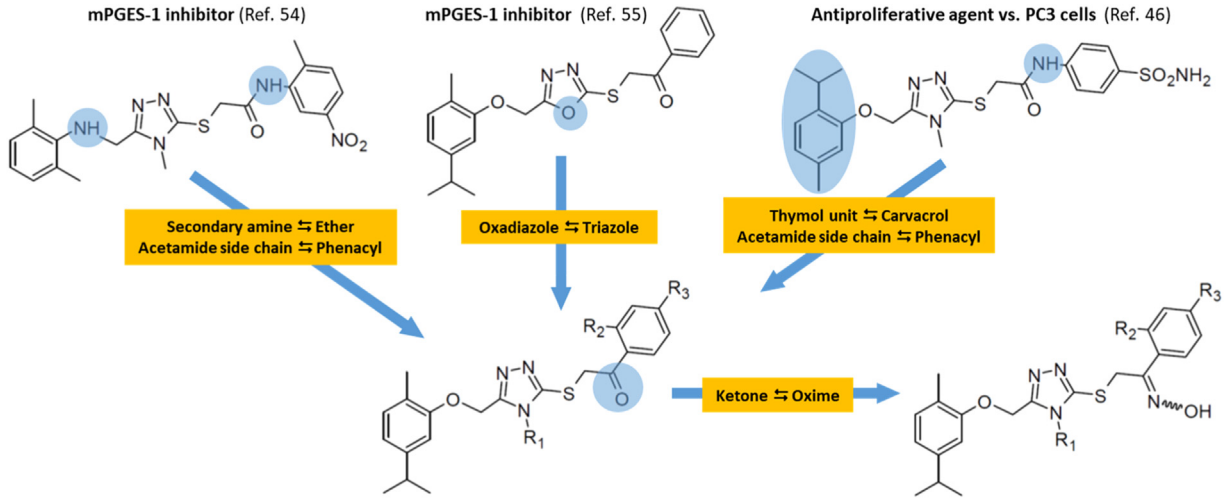

Fig. 1. Design strategy of the new mPGES-1 inhibitors.

2.1.2. Synthesis of compound 2

Compound **1** (0.03 mol) and hydrazine hydrate (0.06 mol) in 20 mL ethanol refluxed for 2 h. Then the solution was cooled, filtered, dried and recrystallized from ethanol:water mixture [56]. HPLC t_R (min): 4.38, M.p: 128–130 °C, TLC $R_{f:}$ 0.29 (S1), yield 73%. IR ν: 3309 and 3200 (N–H str), 1666 (C=O), ^{1}H NMR (300 MHz, DMSO–d_6): δ 1.17 (d, 6H, $J = 6.9$ *Hz*, –CH(C**H$_3$**)$_2$); 2.14 (s, 3H, Ar-C**H$_3$**); 2.80 (septet, 1H, $J = 6.9$ *Hz*, –C**H**(CH$_3$)$_2$); 4.34 (s, 2H, –N**H$_2$**–); 4.48 (s, 2H, –S–CH$_2$–); 6.72–6.74 (m, 2H, Ar-**H**); 7.04 (d, 1H, $J = 8.1$ *Hz*, Ar-**H**); 9.20 (s, 1H, CO–N**H**–). Anal. Calcd. for $C_{12}H_{18}N_2O_2$: C, 64.84; H, 8.16; N,12.60. Found: C, 63.34; H, 7.49; N, 12.35.

2.1.3. General synthesis of compounds 3 and 4

A mixture of compound **2** (0.03 mol) and ethyl/methyl isothiocyanate (0.03 mol) in ethanol (40 mL) was heated under reflux for 4 h. Then the solution was cooled, filtered, and recrystallized from ethanol [47].

N-Methyl-2-[2-methyl-5-(propan-2-yl)phenoxy]acetyl] hydrazinecarbothioamide **(3)**. W hite solid. HPLC t_R (min): 5.57, M.p: 178–182 °C, TLC $R_{f:}$0.61 (S1), yield 65%. IR ν: 3374, 3360 and 3170 (N–H str), 1699 (C=O), 1554 (N–H bnd). ^{1}H NMR (300 MHz, DMSO–d_6): δ 1.18 (d, 6H, $J = 6.9$ *Hz*, –CH(C**H$_3$**)$_2$); 2.15 (s, 3H, Ar-C**H$_3$**); 2.81–2.88 (m, 4H, –C**H**(CH$_3$)$_2$, –NH–C**H$_3$**); 4.62 (s, 2H, –S–CH$_2$–); 6.74 (d, $J = 8.1$ *Hz*,2H, Ar–**H**); 7.04 (d, 1H, $J = 7.5$ *Hz*, Ar-**H**); 7.95 (s, 1H, –N**H**–CH$_3$); 9.33 (s, 1H, CONH–N**H**); 9.88 **(**s, 1H, –CON**H**). Anal. Calcd. for $C_{14}H_{21}N_3O_2S$: C, 56.92; H, 7.17; N, 14.22; S, 10.85. Found: C, 56.71; H, 6.60; N, 14.17; S, 10.83.

N-Ethyl-2-[2-methyl-5-(propan-2-yl)phenoxy]acetyl] hydrazinecarbothioamid **(4)**. White solid. HPLC t_R (min): 6.10, M.p: 138–142 °C, TLC $R_{f:}$ 0.30 (S1), yield 62%. IR ν: 3340, 3327 and 3153 (N–H str), 1693 (C=O), 1546 (N–H bnd). ^{1}H NMR (300 MHz, DMSO–d_6): δ 1.05 (t, 3H, $J = 7.2$ *Hz*, –NCH$_2$C**H$_3$**); 1.18 (d, 6H, $J = 6.9$ *Hz*, -CH(C**H$_3$**)$_2$); 2.15 (s, 3H, Ar-C**H$_3$**); 2.82 (septet, 1H, $J = 6.9$ *Hz*, -C**H**(CH$_3$); 3.45 (q, $J = 6.6$ *Hz* 2H,–NC**H$_2$**CH$_3$); 4.60 (s, 2H, –S–CH$_2$–); 6.74 (d, $J = 7.2$ *Hz* 2H, Ar–**H**); 7.05 (d, 1H, $J = 7.5$ *Hz*, Ar-**H**); 7.95 (s, 1H, –N**H**–CH$_2$); 9.26 (s, 1H, CONH–N**H**); 9.88 **(**s, 1H, –CON**H**). Anal. Calcd. for $C_{15}H_{23}N_3O_2S$: C, 58.22; H, 7.49; N,13.58; S, 10.36. Found: C, 58.15; H, 7.28; N, 13.56; S, 10.34.

2.1.4. General synthesis of compounds 5 and 6

Compounds **5** and **6** were obtained by refluxing compound **3** or **4** (0,015 mol) in 2 N NaOH for 4 h. After neutralization with 10% HCl, the solid product was filtered, dried, and recrystallized from ethanol [47].

4-Methyl-5-{[2-methyl-5-(propan-2-yl)phenoxy]methyl}2,4-dihydro-3*H*-1,2,4-triazole-3-thione **(5)**. White solid. HPLC t_R (min): 7.55, M.p: 149–152 °C, TLC $R_{f:}$ 0.51(S2), yield 54%. IR ν: 3157 and 3130 (N–H str), 1614 (C=N), 1585 (N–H bnd), 1276 (C=S) ^{1}H NMR (300 MHz, DMSO–d_6): δ 1.19 (d, 6H, $J = 6.9$ *Hz*, -CH(C**H$_3$**)$_2$); 2.09 (s, 3H, Ar-C**H$_3$**); 2.84 (septet, 1H, $J = 6.9$ *Hz*, -C**H**(CH$_3$)$_2$); 3.51 (s, 3H, –N-C**H$_3$**); 5.22 (s, 2H, –S–CH$_2$–); 6.77 (d, 1H, $J = 7.5$ *Hz*, Ar-**H**), 6.98 (s, 1H, Ar-**H**); 7.05 (d, 1H, $J = 7.8$ *Hz*, Ar-**H**); 13.85 (s, 1H, triazole=N–N**H**–). Anal. Calcd. for $C_{14}H_{19}N_3OS$. ¼ H_2O: C, 59.65; H, 6.97; N, 14.91; S,11.38. Found: C, 59.73; H, 6.45; N, 15.11; S, 10.23.

4-Ethyl-5-methyl}2,4-dihydro-3*H*-1,2,4-triazole-3-thione **(6)**. White solid. HPLC t_R (min): 8.29, M.p: 100–103 °C, TLC $R_{f:}$ 0.57(S2), yield 58%. IR ν: 3089 and 3055 (N–H str), 1615 (C=N), 1576 (N–H bnd), 1277 (C=S). ^{1}H NMR (300 MHz, DMSO–d_6): δ 1.19 (d, 6H, $J = 6.9$ *Hz*, -CH(C**H$_3$**)$_2$); 1.28 (t, 3H, $J = 7.2$ *Hz*, –N-CH$_2$–C**H$_3$**); 2.09 (s, 3H, Ar-C**H$_3$**); 2.82 (septet, 1H, $J = 6.9$ *Hz*, -C**H**(CH$_3$)$_2$); 4.05 (q, 2H, $J = 7.2$ *Hz*, –N-C**H$_2$**–CH$_3$); 5.22 (s, 2H, –S–CH$_2$–); 6.78 (d, 1H, $J = 7.5$ *Hz*, Ar-**H**), 6.99 (s, 1H, Ar-**H**); 7.06 (d, 1H, $J = 7.8$ *Hz*, Ar-**H**); 13.87 (s, 1H, triazole=N–N**H**–). ^{13}C NMR (150- MHz, DMSO–d_6): δ 13.85, 16.11, 24.36, 33.89, 39.31, 60.32, 110.65, 119.40, 123.52, 130.97, 148.07, 152.11 (triazole-C_5), 155.76, 167.57 (C=S). Anal. Calcd. for $C_{15}H_{21}N_3OS$. ½ H_2O: C, 59.97; H, 7.38; N, 13.99; S,10.67. Found: C, 59.71; H, 7.38; N, 13.99; S, 10.67.

2.1.5. General synthesis of compounds 7–18

An equimolar mixture of **5** or **6** and substituted phenacyl bromide (0.01 mol) and TEA (0.012 mol) in acetonitrile (50 mL) was heated at reflux for 4–8 h. The reaction mixture was evaporated to dryness. The residue was crystallized from aqueous ethanol [57].

1-Phenyl-2-[(4-methyl-5-{[2-methyl-5-(propan-2-yl)phenoxy]methyl}–4*H*-1,2,4-triazole-3-yl)sulfanyl]etan-1-one **(7)** White solid. HPLC t_R (min): 9.96, M.p: 119–121 °C, TLC R_f: 0.60(S3), yield 61%. IR ν: 1615 (C=O), 1579 (C=N str), 1203 (C–O-C), 690 (C-S-C). ^{1}H NMR (300 MHz, DMSO–d_6): δ 1.18 (d, 6H, $J = 6.9$ *Hz*, -CH(C**H$_3$**)$_2$); 2.09 (s, 3H, Ar-C**H$_3$**); 2.83 (septet, 1H, 6H, $J = 6.9$ *Hz*, -C**H**(CH$_3$)$_2$); 3.63 (s, 3H, N–C**H$_3$**); 4.93 (s, 2H, -S-C**H$_2$-**); 5.27 (s, 2H, –S–CH$_2$–); 6.76 (dd, 1H, $J = 7.5$ *Hz*, $J = 1.5$ *Hz*, Ar-**H**); 7.03–7.06 (m, 2H, Ar-**H**); 7.55 (t, 2H, $J = 7.5$ *Hz*, $J = 7.8$ *Hz*, Ar-**H**); 7.69 (t, 1H, $J = 7.2$ *Hz*, $J = 7.5$ *Hz*,Ar-**H**); 8.02 (dd, 2H, $J = 7.2$ *Hz*, $J = 1.2$ *Hz*, Ar-**H**). ^{13}C NMR (150 MHz, DMSO–d_6): δ 16.06, 24.37, 30.95, 33.91, 40.80, 60.52, 110.93, 119.22, 123.75, 128.98, 129.29, 130.84, 134.23, 135.69, 148.06, 150.94 (triazole C_3), 152.71 (triazole-C_5), 155.98, 193.71. LR-MS (*m/z*): calculated for $(M+H)^+$:396.174, found: 396, calculated for $(M\text{-}H)^-$:394.159, found: 394. Anal. Calcd. for

$C_{22}H_{25}N_3O_2S$. ½ H_2O: C, 65.32; H, 6.48; N, 10.39; S, 7.93. Found: C, 65.19; H, 6.36; N, 10.53; S, 7.64.

1-(4-Chlorohenyl)−2-[(4-methyl-5-{[2-methyl-5-(propan-2-yl)phenoxy]metlhy}−4*H*-1,2,4-triazole-3-yl)sulfanyl]ethan-1-one **(8)** White solid. HPLC t_R (min): 14.68, M.p: 128–130 °C, TLC R_f: 0.42(S3), yield 77%. IR ν: 1671 (C=O), 1587 (C=N str), 1128 (C–O-C), 679 (C-S-C). ^{1}H NMR (300 MHz, DMSO–d_6): δ 1.18 (d, 6H, *J* = *6.9 Hz,* -CH(C**H$_3$**)$_2$); 2.09 (s, 3H, Ar-C**H$_3$**); 2.84 (septet, 1H, *J* = *6.9 Hz,* -C**H**(CH$_3$)$_2$); 3.63 (s, 3H, N–C**H$_3$**); 4.91 (s, 2H, -S-C**H$_2$-**); 5.27 (s, 2H, −S–CH$_2$−); 6.76 (dd, 1H, *J* = *7.5 Hz, J* = *1.5 Hz,* Ar–**H**); 7.03–7.07 (m, 2H, Ar-**H**); 7.64 (dd, 2H, *J* = *6.9 Hz, J* = *1.8 Hz*, Ar-**H**); 8.03 (dd, 2H, *J* = *6.9 Hz, J* = *1.8 Hz,* Ar–**H**). ^{13}C NMR (150 MHz, DMSO–d_6): δ 16.03, 24.37, 30.93, 33.90, 40.95, 60.55, 110.96, 119.22, 123.76, 129.40, 130.81, 130.84, 134.42, 135.69, 148.06, 150.81 (triazole C_3), 152.75 (triazole-C_5), 155.98, 192.86. LR-MS (*m/z*): calculated for $(M+H)^+$:430.135, found: 430, calculated for (M-H)$^-$: 428.120, found: 428. Anal. Calcd. for $C_{22}H_{24}ClN_3O_2S$. ¼ H_2O: C, 60.82; H, 5.68; N, 9.67; S, 7.38. Found: C, 60.15; H, 5.81; N, 9.67; S, 7.73.

1-(3,4-Dichlorophenyl)−2-[(4-methyl-5-{[2-methyl-5-(propan-2-yl)phenoxy]metlhy}−4H-1,2,4-triazole-3-yl)sulfanyl]ethan-1-one **(9)** White solid. HPLC t_R (min): 17.72, M.p: 113–117 °C, TLC R_f: 0.30 (S3), yield 74%. IR ν: 3089, 3065 (Ar C–H str), 1686 (C=O), 1571 (C=N str), 1199 (C–O-C), 691 (C-S-C). ^{1}H NMR (300 MHz, DMSO–d_6): δ 1.19 (d, 6H, *J* = *6.9 Hz,* -CH(C**H$_3$**)$_2$); 2.09 (s, 3H, Ar-C**H$_3$**); 2.84 (septet, 1H, *J* = *6.9 Hz,* -C**H**(CH$_3$)$_2$); 3.63 (s, 3H, N–C**H$_3$**); 4.91 (s, 2H, -S-C**H$_2$-**); 5.27 (s, 2H, −S–CH$_2$−); 6.76 (dd, 1H, *J* = *7.5 Hz, J* = *1.2 Hz* Ar-**H**); 7.02–7.06 (m, 2H, Ar-**H**); 7.84 (d, 1H, *J* = *8.4 Hz*, Ar-**H**); 7.97 (dd, 1H, *J* = *8.4 Hz, J* = *2.1 Hz*, Ar-**H**); 8.25 (d, 1H, *J* = *2.1 Hz,* Ar-**H**). LR-MS (*m/z*): calculated for $(M+H)^+$:464.096, found: 464, calculated for (M-H)$^-$: 462.081, found: 462. Anal. Calcd. for $C_{22}H_{23}Cl_2N_3O_2S$. ½ H_2O: C, 55.81; H, 5.11; N, 8.88; S, 6.77. Found: C, 55.34; H, 5.24; N, 8.94; S, 7.41.

1-(4-Fluorophenyl)−2-[(4-methyl-5-{[2-methyl-*5-(*propan-*2-*yl*)*phenoxy*]metlhy}−4H-1,2,4-triazole-3-yl)*sulfanyl]ethan-1-one **(10)** White solid. HPLC t_R (min): 11.35, M.p: 136–138 °C, TLC R_f: 0.23 (S3), yield 65%. IR ν: 1678 (C=O), 1593 (C=N str), 1159 (C–O-C), 678 (C-S-C). ^{1}H NMR (300 MHz, DMSO–d_6): δ 1.19 (d, 6H, *J* = *6.9 Hz* -CH(C**H$_3$**)$_2$); 2.09 (s, 3H, Ar-C**H$_3$**); 2.84 (septet, 1H, *J* = *6.9 Hz* -C**H**(CH$_3$)$_2$); 3.63 (s, 3H, N–C**H$_3$**); 4.91 (s, 2H, -S-C**H$_2$-**); 5.27 (s, 2H, −S–CH$_2$−); 6.75 (d, 1H, *J* = *7.5 Hz,* Ar-**H**); 7.03–7.07 (m, 2H, Ar-**H**); 7.39 (t, 2H, *J* = *9 Hz*, Ar-**H**); 8.11 (dd, 2H, *J* = *9 Hz, J* = *5.4 Hz,* Ar-**H**). LR-MS (*m/z*): calculated for $(M+H)^+$: 414.165, found: 414, calculated for (M-H)$^-$: 412.150, found: 412. Anal. Calcd. for $C_{22}H_{24}FN_3O_2S$. ½ H_2O: C, 62.54; H, 5.96; N, 9.95; S, 7.59. Found: C, 62.40; H, 5.86; N, 10.09; S, 7.86.

1-(4-Methoxyphenyl)−2-[(4-methyl-5-{[2-methyl-5-(propan-2-yl)phenoxy]metlhy}−4*H*-1,2,4-triazole-3-yl)sulfanyl]ethan-1-one **(11)** White solid. HPLC t_R (min): 9.84, M.p: 72–75 °C, TLC R_f: 0.30 (S3), yield 61%. IR ν: 3312 and 3213 (Ar C–H str), 1689 (C=O), 1598 (C=N str), 1179 (C–O-C), 689 (C-S-C). ^{1}H NMR (300 MHz, DMSO–d_6): δ 1.19 (d, 6H, *J* = *6.9 Hz* -CH(C**H$_3$**)$_2$); 2.09 (s, 3H, Ar-C**H$_3$**); 2.84 (septet, 1H, *J* = *6.9 Hz*, -C**H**(CH$_3$)$_2$); 3.63 (s, 3H, N–C**H$_3$**); 3.86 (s, 3H, Ar–OC**H$_3$**); 4.86 (s, 2H, -S-C**H$_2$-**); 5.27 (s, 2H, −S–CH$_2$−); 6.76 (d, 1H, *J* = *7.5 Hz,* Ar-**H**); 7.04–7.011 (m, 4H, Ar-**H**); 8.09 (d, 2H, *J* = *9.0 Hz,* Ar-**H**). LR-MS (*m/z*): calculated for $(M+H)^+$: 426.185, found: 426, calculated for (M-H)$^-$: 424.170, found: 424. Anal. Calcd. for $C_{23}H_{27}N_3O_3S$: C, 64.92; H, 6.40; N, 9.87; S, 7.54. Found: C, 64.88; H, 6.46; N, 9.43; S, 7.48.

1-(4-Bromophenyl)−2-[(4-methyl-5-{[2-methyl-5-(propan-2-yl)phenoxy]metlhy}−4*H*-1,2,4-triazole-3-yl)sulfanyl]ethan-1-one **(12)** White solid. HPLC t_R (min): 15.79, M.p: 122–124 °C, TLC R_f: 0.35 (S3), yield 66%. IR ν: 3086 (Ar C–H str), 1678 (C=O), 1583 (C=N str), 1178 (C–O-C), 678 (C-S-C). ^{1}H NMR (300 MHz, DMSO–d_6): δ 1.18 (d, 6H, *J* = *6.9 Hz,* -CH(C**H$_3$**)$_2$); 2.09 (s, 3H, Ar-C**H$_3$**); 2.85 (septet, 1H, *J* = *6.9 Hz* -C**H**(CH$_3$)$_2$); 3.63 (s, 3H, N–C**H$_3$**); 4.90 (s, 2H, -S-C**H$_2$-**); 5.27 (s, 2H, −S–CH$_2$−); 6.76 (dd, 1H, *J* = *7.5 Hz, J* = *1.5 Hz,* Ar-**H**); 7.03–7.06 (m, 2H, Ar-**H**); 7.77 (d, 2H, *J* = *8.7 Hz*, Ar-**H**); 7.95 (d, 2H, *J* = *8.7 Hz,* Ar-**H**). ^{13}C NMR (75 MHz, DMSO–d_6): δ 16.65, 24.38, 30.93, 33.90, 40.83, 60.51, 110.92, 119.21, 123.74, 128.37, 130.82, 130.89, 132.35, 134.72, 148.04, 150.81 (triazole C_3), 152.73 (triazole-C_5), 155.96, 193.06. LR-MS (*m/z*): calculated for $(M+H)^+$: 474.084, found: 474, calculated for (M-H)$^-$: 472.070, found: 472. Anal. Calcd. for $C_{22}H_{24}BrN_3O_2S$: C, 55.70; H, 5.10; N, 8.86; S, 6.76. Found: C, 55.37; H, 5.14; N, 8.87; S, 7.69.

1-Phenyl-2-[(4-ethyl-5-{[2-methyl-5-(propan-2-yl)phenoxy]metlhy}−4*H*-1,2,4-triazole-3-yl)sulfanyl]ethan-1-one **(13)** Off-white solid. HPLC t_R (min): 12.62, M.p: 116–118 °C, TLC R_f: 0.28 (S3), yield 66%. IR ν: 3070 (Ar C–H str), 1681 (C=O), 1593 (C=N str), 1176 (C–O-C), 686 (C-S-C). ^{1}H NMR (300 MHz, DMSO–d_6): δ 1.19 (d, 6H, *J* = *6.9 Hz,* -CH(C**H$_3$**)$_2$); 1.32 (t, 3H, *J* = *7.2 Hz*, N–CH$_2$–C**H$_3$**); 2.09 (s, 3H, Ar-C**H$_3$**); 2.84 (septet, 1H, *J* = *6.9 Hz,* -C**H**(CH$_3$)$_2$); 4.01 (q, 2H, *J* = *7.2 Hz*, N–CH$_2$–C**H$_3$**); 4.99 (s, 2H, -S-C**H$_2$-**); 5.27 (s, 2H, −S–CH$_2$−); 6.76 (dd, 1H, *J* = *7.8 Hz, J* = *1.2 Hz,* Ar-**H**); 7.04–7.07 (m, 2H, Ar-**H**); 7.55 (t, 2H, *J* = *7.2 Hz*, Ar-**H**); 7.69 (t, 1H, *J* = *7.5 Hz,* Ar-**H**); 8.03 (dd, 2H, *J* = *7.2 Hz, J* = *1.2 Hz,* Ar-**H**). LR-MS (*m/z*): calculated for $(M+H)^+$: 410.190, found: 411, calculated for (M-H)$^-$: 408.175, found: 408. Anal. Calcd. for $C_{23}H_{27}N_3O_2S$: C, 67.45; H, 6.65; N, 10.26; S, 7.83. Found: C, 67.10; H, 6.61; N, 9.80; S, 8.10.

1-(4-Chlorophenyl)−2-[(4-ethyl-5-{[2-methyl-5-(propan-2-yl)phenoxy]metlhy}−4*H*-1,2,4-triazole-3-yl)sulfanyl]ethan-1-one **(14)** White solid. HPLC t_R (min): 16.98, M.p: 131–133 °C, TLC R_f: 0.30 (S3), yield 83%. IR ν: 3100 (Ar C–H str), 1681 (C=O), 1590 (C=N str), 1199 (C–O-C), 690 (C-S-C). ^{1}H NMR (300 MHz, DMSO–d_6): δ 1.19 (d, 6H, *J* = *6.9 Hz,* -CH(C**H$_3$**)$_2$); 1.32 (t, 3H, *J* = *7.2 Hz*, N–CH$_2$–C**H$_3$**); 2.09 (s, 3H, Ar-C**H$_3$**); 2.84 (septet, 1H, *J* = *6.9 Hz,* -C**H**(CH$_3$)$_2$); 4.09 (q, 2H, *J* = *7.2 Hz*, N–CH$_2$–C**H$_3$**); 4.98 (s, 2H, -S-C**H$_2$-**); 5.27 (s, 2H, −S–CH$_2$−); 6.77 (d, 1H, *J* = *7.8 Hz,* Ar-**H**); 7.04–7.07 (m, 2H, Ar-**H**); 7.63 (dd, 2H, *J* = *9 Hz, J* = *2.1 Hz*, Ar-**H**); 8.04 (dd, 2H, *J* = *9 Hz, J* = *2.1 Hz,* Ar-**H**). ^{13}C NMR (75 MHz, DMSO–d_6): δ 15.57, 16.17, 24.38, 33.91, 40.81, 60.23, 110.69, 119.12, 123.44, 129.41, 130.81, 130.86, 134.72, 139.14, 148.06, 150.32 (triazole C_3), 152.12 (triazole-C_5), 156.61, 192.75. LR-MS (*m/z*): calculated for $(M+H)^+$: 444.151, found: 444, calculated for (M-H)$^-$: 442.136, found: 442. Anal. Calcd. for $C_{23}H_{26}ClN_3O_2S$. ½ H_2O: C, 60.98; H, 6.01; N, 9.28; S, 7.08. Found: C, 60.67; H, 5.89; N, 9.33; S, 6.08.

1-(3,4-Dichlorophenyl)−2-[(4-ethyl-5-{[2-methyl-5-(propan-2-yl)phenoxy]metlhy}−4*H*-1,2,4-triazole-3-yl)sulfanyl]ethan-1-one **(15)** White solid. HPLC t_R (min): 23.33, M.p: 124–126 ^{0}C, TLC R_f: 0.16 (S3), yield 87%. IR ν: 3100, 3086 (Ar C–H str), 1686 (C=O), 1583 (C=N str), 1193 (C–O-C), 695 (C-S-C). ^{1}H NMR (300 MHz, DMSO–d_6): δ 1.19 (d, 6H, *J* = *6.9 Hz,* -CH(C**H$_3$**)$_2$); 1.33 (t, 3H, *J* = *7.2 Hz*, N–CH$_2$–C**H$_3$**); 2.09 (s, 3H, Ar-C**H$_3$**); 2.84 (septet, 1H, *J* = *6.9 Hz,* -C**H**(CH$_3$)$_2$); 4.09 (q, 2H, *J* = *7.2 Hz*, N–CH$_2$–C**H$_3$**); 4.99 (s, 2H, -S-C**H$_2$-**); 5.27 (s, 2H, −S–CH$_2$−); 6.77 (dd, 1H, *J* = *7.5 Hz, J* = *1.2 Hz,* Ar-**H**); 7.04–7.07 (m, 2H, Ar-**H**); 7.85 (d, 1H, *J* = *8.4 Hz*, Ar-**H**); 7.98 (dd, 1H, *J* = *8.4 Hz, J* = *2.1 Hz,* Ar-**H**); 8.25 (d, 1H, *J* = *2.1 Hz,* Ar-**H**). ^{13}C NMR (75 MHz, DMSO–d_6): δ 15.58, 16.16, 24.37, 33.91, 40.81, 60.23, 110.69, 119.11, 123.44, 128.37, 130.82, 130.86, 131.62, 132.36, 135.95, 137.02, 148.05, 150.17 (triazole C_3), 152.16 (triazole-C_5), 156.01, 192.09. LR-MS (*m/z*): calculated for $(M+H)^+$: 478.117, found: 478. calculated for (M-H)$^-$: 476.097, found: 476, Anal. Calcd. for $C_{23}H_{25}Cl_2N_3O_2S$. ½ H_2O: C, 56.67; H, 5.38; N, 8.62; S, 6.58. Found: C, 56.61; H, 5.57; N, 8.58; S, 6.00.

1-(4-Fluorophenyl)−2-[(4-ethyl-5-{[2-methyl-5-(propan-2-yl)phenoxy]metlhy}−4*H*-1,2,4-triazole-3-yl)sulfanyl]ethan-1-one **(16)** White solid. HPLC t_R (min): 13.01, M.p: 134–137 °C, TLC R_f: 0.33 (S3), yield 63%. IR ν: 3100 and 3061 (Ar C–H str), 1676 (C=O), 1593 (C=N str), 1224 (C–O-C), 691 (C-S-C). ^{1}H NMR (300 MHz, DMSO–d_6): δ 1.19 (d, 6H, *J* = *6.9 Hz,* -CH(C**H$_3$**)$_2$); 1.33 (t, 3H, *J* = *7.2 Hz*, N–CH$_2$–C**H$_3$**); 2.09 (s, 3H, Ar-C**H$_3$**); 2.84 (septet, 1H,

J = 6.9 Hz, -C**H**$(CH_3)_2$); 4.09 (q, 2H, *J* = 7.2 Hz, N–CH_2–C**H$_3$**); 4.99 (s, 2H, -S-C**H$_2$-**); 5.27 (s, 2H, –S–CH_2–); 6.77 (d, 1H, *J* = 7.5 Hz, Ar-**H**); 7.05–7.07 (m, 2H, Ar-**H**); 7.39 (t, 2H, *J* = 9 Hz, Ar-**H**); 8.12 (dd, 2H, *J* = 9 Hz, *J* = 5.7 Hz, Ar-**H**). ^{13}C NMR (150 MHz, DMSO–d_6): *δ* 15.58, 16.17, 24.38, 33.92, 39.66, 40.89, 60.23, 110.69, 116.28–116.43 (d, *J* = 22.5 Hz), 119.12, 123.45, 130.87, 131.62–132.01 (d, *J* = 9 Hz), 132.52–132.54 (d, *J* = 3 Hz), 148.08, 150.39 (triazole C_3), 152.11 (triazole-C_5), 156.02, 164.94–166.62 (d, *J* = 252 Hz), 192.28. LR-MS (*m/z*): calculated for $(M+H)^+$: 428.180, found: 429, calculated for $(M\text{-}H)^-$: 426.166, found: 426. Anal. Calcd. for $C_{23}H_{26}FN_3O_2S$. ¾ H_2O: C, 62.63; H, 6.28; N, 9.53; S, 7.27. Found: C, 62.97; H, 6.08; N, 9.71; S, 7.56.

1-(4-Methoxyphenyl)−2-[(4-ethyl-5-{[2-methyl-5-(propan-2-yl)phenoxy]metlhy}−4H-1,2,4-triazole-3-yl)sulfanyl]ethan-1-one **(17)** White solid. HPLC t_R (min): 12.46, M.p: 100–104 ^{0}C, TLC R_f: 0.5(S3), yield 64%. IR *ν*: 3086, 3006 (Ar C–H str), 1664 (C=O), 1597 (C=N str), 1201 (C–O-C), 697 (C-S-C). ^{1}H NMR (300 MHz, DMSO–d_6): *δ* 1.19 (d, 6H, *J* = 6.9 Hz, -CH(C**H$_3$**)$_2$); 1.32 (t, 3H, *J* = 7.2 Hz, N–CH_2–C**H$_3$**); 2.09 (s, 3H, Ar-C**H$_3$**); 2.84 (septet, 1H, *J* = 6.9 Hz, -C**H**$(CH_3)_2$); 3.86 (s, 3H, –OC**H$_3$**); 4.09 (q, 2H, *J* = 7.2 Hz, N–CH_2–C**H$_3$**); 4.94 (s, 2H, -S-C**H$_2$-**); 5.27 (s, 2H, –S–CH_2–); 6.76 (d, 1H, *J* = 7.5 Hz, Ar-**H**); 7.05–7.09 (m, 4H, Ar-**H**); 8.00 (d, 2H, *J* = 9.0 Hz, Ar-**H**). LR-MS (*m/z*): calculated for $(M+H)^+$: 440.200, found: 440, calculated for $(M\text{-}H)^-$: 438.186, found: 438. Anal. Calcd. for $C_{24}H_{29}N_3O_3S$. ½ H_2O: C, 64.26; H, 6.74; N, 9.37; S, 7.15. Found: C, 64.37; H, 6.70; N, 9.59; S, 7.45.

1-(4-Bromophenyl)−2-[(4-ethyl-5-{[2-methyl-5-(propan-2-yl)phenoxy]metlhy}−4H-1,2,4-triazole-3-yl)sulfanyl]ethan-1-one **(18)** White solid. HPLC t_R (min): 18.25, M.p: 131–133 °C, TLC R_f: 0.35 (S3), yield 83%. IR cm $^{-1}$: 3066 (Ar C–H str), 1681 (C=O), 1585 (C=N str), 1208 (C–O-C), 689 (C-S-C). ^{1}H NMR (300 MHz, DMSO–d_6): *δ* 1.19 (d, 6H, *J* = 6.9 Hz, -CH(C**H$_3$**)$_2$); 1.33 (t, 3H, *J* = 7.2 Hz, N–CH_2–C**H$_3$**); 2.09 (s, 3H, Ar-C**H$_3$**); 2.84 (septet, 1H, *J* = 6.9 Hz, -C**H**$(CH_3)_2$); 4.09 (q, 2H, *J* = 7.2 Hz, N–CH_2–C**H$_3$**); 4.97 (s, 2H, -S-C**H$_2$-**); 5.27 (s, 2H, –S–CH_2–); 6.77 (d, 1H, *J* = 7.5 Hz, Ar-**H**); 7.04–7.07 (m, 2H, Ar-**H**); 7.78 (dd, 2H, *J* = 6.9 Hz, *J* = 1.8 Hz, Ar-**H**); 7.96 (dd, 2H, *J* = 6.9 Hz, *J* = 1.8 Hz, Ar-**H**). LR-MS (*m/z*): calculated for $(M+H)^+$: 488.100, found: 488, calculated for $(M\text{-}H)^-$: 486.086, found: 486. Anal. Calcd. for $C_{23}H_{26}BrN_3O_2S$. 3/4 H_2O: C, 55.03; H, 5.52; N, 8.77; S, 6.39. Found: C, 54.88; H, 5.33; N, 8.47; S, 5.65.

2.1.6. General synthesis of compounds 19–30

A mixture of equimolar amounts of the appropriate ketone derivatives (**7–18**) (0.01 mol) and hydroxylamine hydrochloride (0.03 mol) in absolute ethanol (30 mL) in presence of pyridine (0.03 mol) was heated under reflux for 8–24 h. The mixture was poured onto the crushed ice and the precipitated solid was washed with distilled water, dried, and recrystallized from ethanol [57].

2-{[3-[1-[5-Methyl-2-(propan-2-yl)phenoxy]methyl]−4-methyl-4*H*-1,2,4-triazole-3-yl]sulfanyl}−1-(phenyl)ethanone oxime (**19**) Whitesolid. HPLC t_R (min): 7.63; M.p: 176–178 ^{0}C, TLC R_f: 0.54 (S3), yield 86%. IR *ν*: 3128 (=*N*–OH str), 1610 (C=O), 1587 (C=N str), 950 (N–O); 680 (C-S-C). ^{1}H NMR (300 MHz, DMSO–d_6): *δ* 1.20 (d, 6H, *J* = 6.9 Hz, -CH(C**H$_3$**)$_2$); 2.07 (s, 3H, Ar-C**H$_3$**); 2.85 (septet, 1H, *J* = 6.9 Hz,-C**H**$(CH_3)_2$); 3.53 (s, 3H, N–C**H$_3$**); 4.40 (s, 2H, -S-C**H$_2$-**); 5.25 (s, 2H, –S–CH_2–); 6.77 (dd, 1H, *J* = 7.5 Hz, *J* = 1.2 Hz, Ar-**H**); 7.04–7.06 (m, 2H, Ar-**H**); 7.34–7.39 (m, 3H, Ar-**H**); 7.62–7.68 (m, 2H, Ar-**H**); 11.82 (s, 1H, =*N*–O**H**). ^{13}C NMR (150 MHz, DMSO–d_6): *δ* 16.01, 24.39, 26.34, 30.88, 33.91, 60.59, 110.87, 119.20, 123.77, 126.88, 128.94, 129.57, 130.82, 134.15, 148.06, 150.78 (triazole C_3), 152.62 (C=N), 152.91 (triazole-C_5), 155.98. LR-MS (*m/z*): calculated for $(M+H)^+$: 411.185, found: 411, calculated for $(M\text{-}H)^-$: 409.170, found: 276. Anal. Calcd. for $C_{22}H_{26}N_4O_2S$: C, 64.36; H, 6.38; N, 13.65; S, 7.81. Found: C, 63.75; H, 6.03; N, 13.40; S, 7.60.

2-{[3-[1-[5-Methyl-2-(propan-2-yl)phenoxy]methyl]−4-methyl-4*H*-1,2,4-triazole-3-yl]sulfanyl}−1-(4-chlorophenyl)ethanone oxime (**20**) White solid. HPLC t_R (min): 10.15; M.p: 185–186 °C, TLC R_f: 0.65 (S3), yield 25%. IR *ν*: 3159 (=*N*–OH str), 1608 (C=O), 1577 (C=N str), 956 (N–O); 682 (C-S-C). ^{1}H NMR (300 MHz, DMSO–d_6): *δ* 1.19 (d, 6H, *J* = 6.9 Hz, -CH(C**H$_3$**)$_2$); 2.07 (s, 3H, Ar-C**H$_3$**); 2.84 (septet, 1H, *J* = 6.9 Hz,-C**H**$(CH_3)_2$); 3.54 (s, 3H, N–C**H$_3$**); 4.38 (s, 2H, -S-C**H$_2$-**); 5.25 (s, 2H, –S–CH_2–); 6.77 (dd, 1H, *J* = 7.5 Hz, *J* = 1.2 Hz, Ar-**H**); 7.04–7.06 (m, 2H, Ar-**H**); 7.42 (d, 2H, *J* = 8.7 Hz, Ar-**H**); 7.66 (d, 2H, *J* = 9.0 Hz, Ar-**H**); 11.92 (s, 1H, =*N*–O**H**). LR-MS (*m/z*): calculated for $(M+H)^+$: 445.146, found: 445, calculated for $(M\text{-}H)^-$: 443.131, found: 443, 276. Anal. Calcd. for $C_{22}H_{25}ClN_4O_2S$. ½ H_2O: C, 58.20; H, 5.77; N, 12.34; S, 7.06. Found: C, 58.40; H, 5.49; N, 12.50; S, 7.02.

2-{[3-[1-[5-Methyl-2-(propan-2-yl)phenoxy]methyl]−4-methyl-4*H*-1,2,4-triazole-3-yl]sulfanyl}−1-(3,4-dichlorophenyl)ethanone oxime (**21**) White solid. HPLC t_R (min): 13.46; M.p: 171–172 °C, TLC R_f: 0.73 (S3), yield 34%. IR *ν*: 3140 = *N*–OH str), 1610 (C=O), 1581 (C=N str), 952 (N–O); 693 (C-S-C). ^{1}H NMR (300 MHz, DMSO–d_6): *δ* 1.19 (d, 6H, *J* = 6.9 Hz, -CH(C**H$_3$**)$_2$); 2.08 (s, 3H, Ar-C**H$_3$**); 2.84 (septet, 1H, *J* = 6.9 Hz, -C**H**$(CH_3)_2$); 3.56 (s, 3H, N–C**H$_3$**); 4.38 (s, 2H, -S-C**H$_2$-**); 5.25 (s, 2H, –S–CH_2–); 6.76 (dd, 1H, *J* = 7.5 Hz, *J* = 1.2 Hz, Ar-**H**); 7.03–7.06 (m, 2H, Ar-**H**); 7.63–7.64 (m, 2H, Ar-**H**); 7.87–7.90 (m, 1H, Ar-**H**); 12.07 (s, 1H, =*N*–O**H**). LR-MS (*m/z*): calculated for $(M+H)^+$: 479.107, found: 479, 481 $[M+2]^+$, calculated for $(M\text{-}H)^-$: 477.092, found: 477, 276. Anal. Calcd. for $C_{22}H_{24}Cl_2N_4O_2S$: C, 55.12; H, 5.05; N, 11.69; S, 6.69. Found: C, 54.70; H, 4.88; N, 11.55; S, 6.58.

2-{[3-[1-[5-Methyl-2-(propan-2-*yl*)phenoxy]methyl]−4-methyl-4*H*-1,2,4-triazole-3-yl]sulfanyl}−1-(4-fluorophenyl)ethanone oxime (**22**) White solid. HPLC t_R (min): 8.06; M.p: 190–192 ^{0}C, TLC R_f: 0.67 (S3), yield 47%. IR *ν*: 3160 (=*N*–OH str), 1608 (C=O), 1587 (C=N str), 952 (N–O); 702 (C-S-C). ^{1}H NMR (300 MHz, DMSO–d_6): *δ* 1.19 (d, 6H, *J* = 6.9 Hz, -CH(C**H$_3$**)$_2$); 2.07 (s, 3H, Ar-C**H$_3$**); 2.85 (septet, 1H, *J* = 6.9 Hz, -C**H**$(CH_3)_2$); 3.54 (s, 3H, N–C**H$_3$**); 4.39 (s, 2H, -S-C**H$_2$-**); 5.25 (s, 2H, –S–CH_2–); 6.76 (dd, 1H, *J* = 7.5 Hz, *J* = 1.2 Hz, Ar-**H**); 7.03–7.06 (m, 2H, Ar-**H**); 7.20 (t, 2H, *J* = 9.0 Hz, Ar-**H**); 7.70 (dd, 2H, *J* = 7.8 Hz, *J* = 5.4 Hz Ar-**H**); 11.82 (s, 1H, =*N*–O**H**). LR-MS (*m/z*): calculated for $(M+H)^+$: 429.175, found: 429, calculated for $(M\text{-}H)^-$: 427.161, found: 276. Anal. Calcd. for $C_{22}H_{25}FN_4O_2S$: C, 61.66; H, 5.88; N, 13.07; S, 7.48. Found: C, 61.15; H, 5.69; N, 12.87; S, 7.42.

2-{[3-[1-[5-Methyl-2-(propan-2-yl)phenoxy]methyl]−4-methyl-4*H*-1,2,4-triazole-3-yl]sulfanyl}−1-(4-methoxyphenyl)ethanone oxime (**23**) White solid. HPLC t_R (min): 7.48; M.p: 160–162 ^{0}C, TLC R_f: 0.53 (S3), yield 49%. IR *ν*: 3150 (=*N*–OH str), 1606 (C=O), 1575 (C=N str), 950 (N–O); 680 (C-S-C). ^{1}H NMR (300 MHz, DMSO–d_6): *δ* 1.19 (d, 6H, *J* = 6.9 Hz, -CH(C**H$_3$**)$_2$); 2.07 (s, 3H, Ar-C**H$_3$**); 2.85 (septet, 1H, *J* = 6.9 Hz, -C**H**$(CH_3)_2$); 3.54 (s, 3H, N–C**H$_3$**); 3.77 (s, 3H, –OC**H$_3$**); 4.37 (s, 2H, -S-C**H$_2$-**); 5.25 (s, 2H, –S–CH_2–); 6.76 (dd, 1H, *J* = 7.5 Hz, *J* = 1.5 Hz, Ar-**H**); 6.94 ppm (d, 2H, *J* = 9 Hz, Ar-**H**); 7.03–7.06 (m, 2H, Ar-**H**); 7.61 (d, 2H, *J* = 9 Hz, Ar-**H**); 11.60 (s, 1H, =*N*–O**H**). ^{13}C NMR (150 MHz, DMSO–d_6): *δ* 16.01, 24.39, 26.21, 30.90, 33.91, 55.65, 60.60, 110.85, 114.39, 119.21, 123.76, 127.11, 127.69, 130.83, 148.05, 150.91 (triazole C_3), 152.16 (C=N), 152.90 (triazole-C_5), 155.97, 160.48. LR-MS (*m/z*): calculated for $(M+H)^+$: 441.195, found: 441, calculated for $(M\text{-}H)^-$: 439.181, found: 276. Anal. Calcd. for $C_{23}H_{28}N_4O_2S$: C, 62.70; H, 6.41; N, 12.72; S, 7.28. Found: C, 62.44; H, 6.17; N, 12.62; S, 7.25.

2-{[3-[1-[5-Methyl-2-(propan-2-yl)phenoxy]methyl]−4-methyl-4*H*-1,2,4-triazole-3-yl]sulfanyl}−1-(4-bromophenyl)ethanone oxime (**24**) White solid. HPLC t_R (min): 10.88; M.p: 180–182 ^{0}C, TLC R_f: 0.65 (S3), yield 22%. IR *ν*: 3100 (=*N*–OH str), 1608 (C=O), 1577 (C=N str), 954 (N–O); 693 (C-S-C). ^{1}H NMR (300 MHz, DMSO–d_6): *δ* 1.19 (d, 6H, *J* = 6.9 Hz, -CH(C**H$_3$**)$_2$); 2.08 (s, 3H, Ar-C**H$_3$**); 2.85 (septet, 1H, *J* = 6.9 Hz, -C**H**$(CH_3)_2$); 3.54 (s, 3H, N–C**H$_3$**); 4.37 (s, 2H, -S-C**H$_2$-**); 5.25 (s, 2H, –S–CH_2–); 6.77 (dd, 1H, *J* = 7.5 Hz, *J* = 1.5 Hz, Ar-**H**); 7.04–7.06 (m, 2H, Ar-**H**); 7.46–7.62 (m, 4H, Ar-**H**); 11.93

(s, 1H, =*N*–O**H**). LR-MS (*m/z*): calculated for $(M+H)^+$: 489.095, found: 489, 491 $[M+2]^+$, calculated for (M-H)$^-$: 487.080, found: 276. Anal. Calcd. for $C_{22}H_{25}BrN_4O_2S$: C, 53.99; H, 5.15; N, 11.45; S, 6.55. Found: C, 53.85; H, 4.78; N, 11.23; S, 6.44.

2-{[3-[1-[5-Methyl-2-(propan-2-yl)phenoxy]methyl]−4-ethyl-4*H*-1,2,4-triazole-3-yl]sulfanyl}−1-(phenyl)ethanone oxime (**25**) White solid. HPLC t_R (min): 9.25; M.p: 131–132 ^{0}C, TLC R_f: 0.62 (S3), yield 41%. IR *ν*: 3182 (=*N*–OH str), 1610 (C=O), 1587 (C=N str), 950 (N–O); 690 (C-S-C). ^{1}H NMR (300 MHz, DMSO–d_6): *δ* 1.19 (m, 9H, -CH(C**H$_3$**)$_2$; −N-CH$_2$−C**H$_3$**); 2.07 (s, 3H, Ar-C**H$_3$**); 2.85 (septet, 1H, *J* = *6.9 Hz*, -C**H**(CH$_3$)$_2$); 3.95 (q, 2H, *J* = *7.2 Hz*, −N-C**H$_2$**−CH$_3$); 4.48 (s, 2H, -S-C**H$_2$**-); 5.26 (s, 2H, −S−CH$_2$−); 6.77 (dd, 1H, *J* = *7.8 Hz, J* = *1.2 Hz*, Ar-**H**); 7.04–7.06 (m, 2H, Ar-**H**); 7.35–7.39 (m, 3H, Ar-**H**); 7.66 (m, 2H, Ar-**H**); 11.88 (s, 1H, =*N*–O**H**). LR-MS (*m/z*): calculated for $(M+H)^+$: 425.200, found: 425, calculated for (M-H)$^-$: 423.186, found: 290. Anal. Calcd. for $C_{23}H_{28}N_4O_2S$: C, 65.07; H, 6.65; N, 13.20; S, 7.55. Found: C, 64.94; H, 6.17; N, 12.62; S, 7.44.

2-{[3-[1-[5-Methyl-2-(propan-2-yl)phenoxy]methyl]−4-ethyl-4*H*-1,2,4-triazole-3-yl]sulfanyl}−1-(4-chlorophenyl)ethanone oxime (**26**) White solid. HPLC t_R (min): 12.73; M.p: 152–154 ^{0}C, TLC R_f: 0.70 (S3), yield 41%. IR *ν*: 3180 (=*N*–OH str), 1612 (C=O), 1575 (C=N str), 964 (N–O); 698 (C-S-C). ^{1}H NMR (300 MHz, DMSO–d_6): *δ* 1.19 (m, 9H, -CH(C**H$_3$**)$_2$; −N-CH$_2$−C**H$_3$**); 2.07 (s, 3H, Ar-C**H$_3$**); 2.85 (septet, 1H, *J* = *6.9 Hz*, -C**H**(CH$_3$)$_2$); 3.98 (q, 2H, *J* = *7.2 Hz*, −N-C**H$_2$**−CH$_3$); 4.46 (s, 2H, -S-C**H$_2$**-); 5.26 (s, 2H, −S−CH$_2$−); 6.77 (dd, 1H, *J* = *7.8 Hz, J* = *1.5 Hz*, Ar-**H**); 7.04–7.06 (m, 2H, Ar-**H**); 7.43 (d, 2H, *J* = *9 Hz*, Ar-**H**); 7.67 (d, 2H, *J* = *9 Hz*, Ar-**H**); 11.98 (s, 1H, =*N*–O**H**). ^{13}C NMR (75 MHz, DMSO–d_6) *δ* 15.64, 16.13, 24.38, 26.29, 33.92, 39.14, 60.27, 110.61, 119.12, 123.44, 128.07, 128.99, 130.87, 133.62, 134.29, 148.05, 150.22 (triazole C_3), 152.88 (C=N), 152.31 (triazole-C_5), 155.99. LR-MS (*m/z*): calculated for $(M+H)^+$: 459.162, found: 459, calculated for (M-H)$^-$: 457.147, found: 457, 290. Anal. Calcd. for $C_{23}H_{27}ClN_4O_2S$: C, 60.18; H, 5.93; N, 12.21; S, 6.99. Found: C, 60.19; H, 5.70; N, 12.14; S, 6.98.

2-{[3-[1-[5-Methyl-2-(propan-2-yl)phenoxy]methyl]−4-ethyl-4*H*-1,2,4-triazole-3-yl]sulfanyl}−1-(3,4-dichlorophenyl)ethanone oxime (**27**) White solid. HPLC t_R (min): 17.25; M.p: 125–127 ^{0}C, TLC R_f: 0.58 (S3), yield 41%. IR *ν*: 3099 (=*N*–OH str), 1616 (C=O), 1585 (C=N str), 983 (N–O); 696 (C-S-C). ^{1}H NMR (300 MHz, DMSO–d_6): *δ* 1.22 (m, 9H, -CH(C**H$_3$**)$_2$;−N-CH$_2$−C**H$_3$**); 2.06 (s, 3H, Ar-C**H$_3$**); 2.85 (septet, 1H, *J* = *6.9 Hz*, -C**H**(CH$_3$)$_2$); 4.01 (q, 2H, *J* = *7.2 Hz*, −N-C**H$_2$**−CH$_3$); 4.46 (s, 2H, -S-C**H$_2$**-); 5.26 (s, 2H, −S−CH$_2$−); 6.77 (dd, 1H, *J* = *7.8 Hz, J* = *1.2 Hz*, Ar-**H**); 7.04–7.06 (m, 2H, Ar-**H**); 7.61–7.67 (m, 2H, Ar-**H**); 7.89–7.90 (m, 1H, Ar-**H**); 12.14 (s, 1H, =*N*–O**H**). ^{13}C NMR (75 MHz, DMSO–d_6): *δ* 15.66, 16.11, 24.38, 26.13, 33.91, 39.14, 60.29, 110.62, 119.12, 123.44, 126.47, 128.07, 128.16, 130.86, 131.13, 131.88, 132.14, 135.43, 148.05, 149.97 (triazole C_3), 151.18 (C=N), 152.36 (triazole-C_5), 155.99. LR-MS (*m/z*): calculated for $(M+H)^+$: 493.123, found: 493, calculated for (M-H)$^-$: 491.108, found: 491, 290. Anal. Calcd. for $C_{23}H_{26}Cl_2N_4O_2S$: C, 55.98; H, 5.31; N, 11.35; S, 6.50. Found: C, 55.54; H, 5.08; N, 11.19; S, 6.47.

2-{[3-[1-[5-Methyl-2-(propan-2-yl)phenoxy]methyl]−4-ethyl-4*H*-1,2,4-triazole-3-yl]sulfanyl}−1-(4-fluorophenyl)ethanone oxime (**28**) White solid. HPLC t_R (min): 9.85; M.p: 141–144 ^{0}C, TLC R_f: 0.68 (S3), yield 41%. IR *ν*: 3166 (=*N*–OH str), 1610 (C=O), 1597 (C=N str), 960 (N–O); 687 (C-S-C). ^{1}H NMR (300 MHz, DMSO–d_6): *δ* 1.22 (m, 9H, -CH(C**H$_3$**)$_2$;−N-CH$_2$−C**H$_3$**); 2.06 (s, 3H, Ar-C**H$_3$**); 2.85 (septet, 1H, *J* = *6.9 Hz*, -C**H**(CH$_3$)$_2$); 3.99 (q, 2H, *J* = *7.2 Hz*, −N-C**H$_2$**−CH$_3$); 4.47 (s, 2H, -S-C**H$_2$**-); 5.26 (s, 2H, −S−CH$_2$−); 6.77 (dd, 1H, *J* = *7.8 Hz, J* = *1.2 Hz*, Ar-**H**); 7.04–7.06 (m, 2H, Ar-**H**); 7.20 (t, 2H, *J* = *9 Hz*, Ar-**H**); 7.71 (dd, 2H, *J* = *9 Hz, J* = *5.4 Hz*, Ar-**H**); 11.88 (s, 1H, =*N*–O**H**). ^{13}C NMR (150 MHz, DMSO–d_6): *δ* 15.62, 16.11, 24.38, 26.43, 33.92, 39.13, 60.26, 110.63, 115,74–116,03 (d, *J* = *21.75 Hz*), 119.11, 123.43, 128.47–128.58 (d, *J* = *8.4 Hz*), 130.86, 131.24–131.28 (d, *J* = *3.2 Hz*), 148.06, 150.31 (triazole C_3), 151.91 (C=N), 152.30 (triazole-C_5), 155.99, 161.53–164.87 (d, *J* = *250.5 Hz*). LR-MS (*m/z*): calculated for $(M+H)^+$: 443.191, found: 443, calculated for (M-H)$^-$: 441.177, found: 290. Anal. Calcd. for $C_{23}H_{27}FN_4O_2S$: C, 62.42; H, 6.15; N, 12.66; S, 7.25. Found: C, 61.67; H, 6.33; N, 12.50; S, 7.15.

2-{[3-[1-[5-Methyl-2-(propan-2-yl)phenoxy]methyl]−4-ethyl-4*H*-1,2,4-triazole-3-yl]sulfanyl}−1-(4-methoxyphenyl)ethanone oxime (**29**) Off-white solid. HPLC t_R (min): 8.92; M.p:155–157 ^{0}C, TLC R_f: 0.65 (S3), yield 63%. IR *ν*: 3140 (=*N*–OH str), 1608 (C=O), 1573(C=N str), 954 (N–O); 690 (C-S-C). ^{1}H NMR (300 MHz, DMSO–d_6): *δ* 1.22 (m, 9H, -CH(C**H$_3$**)$_2$;−N-CH$_2$−C**H$_3$**); 2.07 (s, 3H, Ar-C**H$_3$**); 2.85 (septet, 1H, *J* = *6.9 Hz*, -C**H**(CH$_3$)$_2$); 3.77 (s, 3H, –OC**H$_3$**), 3.99 (q, 2H, *J* = *7.2 Hz*, −N-C**H$_2$**−CH$_3$); 4.45 (s, 2H, -S-C**H$_2$**-); 5.26 (s, 2H, −S−CH$_2$−); 6.76 (dd, 1H, *J* = *7.5 Hz, J* = *1.5 Hz*, Ar-**H**); 6.94 (d, 2H, *J* = *9 Hz*, Ar-**H**), 7.04–7.06 (m, 2H, Ar-**H**); 7.62 (d, 2H, *J* = *9 Hz*, Ar-**H**); 11.66 (s, 1H, =*N*–O**H**). LR-MS (*m/z*): calculated for $(M+H)^+$: 455.211, found: 455, calculated for (M-H)$^-$: 453.197, found: 290. Anal. Calcd. for $C_{24}H_{30}N_4O_3S$: C, 63.41; H, 6.65; N, 12.32; S, 7.05. Found: C, 63.12; H, 6.21; N, 12.33; S, 7.06.

2-{[3-[1-[5-Methyl-2-(propan-2-yl)phenoxy]methyl]−4-ethyl-4*H*-1,2,4-triazole-3-yl]sulfanyl}−1-(4-bromophenyl)ethanone oxime (**30**)White solid. HPLC t_R (min): 8.26; M.p:163–166 ^{0}C, TLC R_f: 0.74 (S3), yield 45%. IR *ν*: 3100 (=*N*–OH str), 1608 (C=O), 1577 (C=N str), 954 (N−−O); 684 (C-S-C). ^{1}H NMR (300 MHz, DMSO–d_6): *δ* 1.20 (m, 9H, -CH(C**H$_3$**)$_2$;−N-CH$_2$−C**H$_3$**); 2.07 (s, 3H, Ar-C**H$_3$**); 2.85 (septet, 1H, *J* = *6.9 Hz*, -C**H**(CH$_3$)$_2$); 3.99 (q, 2H, *J* = *7.2 Hz*, −N-C**H$_2$**−CH$_3$); 4.45 (s, 2H, -S-C**H$_2$**-); 5.26 (s, 2H, −S−CH$_2$−); 6.77 (dd, 1H, *J* = *7.5 Hz, J* = *1.2 Hz*, Ar-**H**); 7.00–7.08 (m, 2H, Ar-**H**); 7.54–7.62 (m, 4H, Ar-**H**); 11.99 (s, 1H, =*N*–O**H**). LR-MS (*m/z*): calculated for $(M+H)^+$: 503.111, found: 503, 505 $[M+2]^+$, calculated for (M-H)$^-$: 501.096, found: 290. Anal. Calcd. for $C_{23}H_{27}BrN_4O_2S$: C, 54.87; H, 5.41; N, 11.13; S, 6.37. Found: C, 54.41; H, 5.76; N, 11.01; S, 6.71.

2.2. Biological methods

2.2.1. Cell culture

Human breast cancer (MCF-7), human lung cancer (A549), human prostate cancer (PC-3), human cervix cancer (HeLa), human chronic myelogenous leukemia (K562), and mouse embryonic fibroblast (NIH/3T3) cells were used. Cells were cultured in Dulbecco's modified eagle medium (DMEM) (Gibco, Rockville, MD, USA) containing 10% fetal bovine serum (FBS) (Gibco, Rockville, MD, USA) and maintained in a 37 °C, 5% CO_2 incubator. Cell passage was conducted at 80–90% confluence.

2.2.2. Cell viability assay

Cell viability was determined by the 3-(4,5-dimethylthiazol-2-yl)−2,5-diphenyltetrazolium bromide (MTT) assay. Briefly, the cells (1×10^4 cells/well) were seeded onto 96-well plates and incubated overnight. Then, the cells were treated with different concentrations (1–50 μM) of compounds for 48 h. After the incubation period, MTT was added to each well to a final concentration of 0.5 mg/mL and incubated for 4 h. The culture medium was then removed and 100μL of the SDS buffer was added to solubilize the purple formazan product. Absorbances at wavelengths of 570 and 630 nm were measured by a microplate reader (BioTek, Winooski, VT, USA).

2.2.3. Measurement of caspase enzymes activities

Caspase-3, 8, and 9 activities were measured by the caspase colorimetric assay kits following the procedure provided by the manufacturer (Millipore, USA). Briefly, treated (50 and 100 μL) and untreated cells were collected after 24 h and resuspended in ready to use chilled lysis buffer for 15 min. Next, centrifugation was performed, and supernatants were collected and used for caspase ac-

tivation assays. Before samples were incubated at 37 °C for 2 h, reaction buffer, DTT and DEVD-p-NA, Ac-IETD-pNA, and Ac-LEHD-pNA substrates for caspase-3, 8, and 9, respectively were added. The principle was that caspase-3 derived from cellular lysate recognizes the sequence Asp-Glu-Val-Asp (DEVD). The assay is based on spectrophotometric detection of the chromophore p-nitroaniline (p-NA) after cleavage from the labelled substrate (DEVD-p-NA). The p-NA light emission can be quantified using a microtiter plate reader at 405 nm. Comparison of the absorbance of p-NA from an apoptotic sample with an untreated control sample allows determination of the fold increase in caspase-3, 8, and 9 activities.

2.2.4. Determination of mitochondrial membrane potential (MMP)

The loss of MMP was detected by JC-1 mitochondrial membrane potential (MMP) kit (MitoPT JC-1, ImmunoChemistry Technologies, LLC). The lipophilic cation JC-1 is widely used in apoptosis studies to monitor mitochondrial health. The membrane-permeant JC-1 dye exhibits potential-dependent accumulation in mitochondria, indicated by a fluorescence emission shift from green (~529 nm) to red (~590 nm). Depending on MMP, JC-1 forms J-aggregates that are associated with a large shift in emission (590 nm). Color dye changes reversibly from orange to green as mitochondrial membranes become depolarized. For JC-1 staining, after the incubation of compounds, cell suspensions were adjusted to a density of 0.5×10^6 cells/ml and incubated in assay buffer with JC-1 (10 µg/ml) for 15 min at 37 °C in the dark. The cells were collected by centrifugation at 1000 rpm for 10 min. Fluorescence intensity at 510 and 585 nm was measured, and the ratio of 585/510 was calculated to determine the changes in MMP.

2.2.5. mPGES-1 and COX-1/2 enzyme inhibition assays

2.2.5.1. Preparation of mPGES-1 enzymes. The cloning of mPGES-1 enzyme and the preparation of protein followed the same protocols as described in our previous reports [58] Briefly, FreeStyle Max Expression system was used to express wild-type human mPGES-1 enzymes. FreeStyle 293-F cells were cultured following the manufacturer's manual in FreeStyle 293 expression medium on orbit rotate shaker in 8% CO_2 incubator at 37 °C. Cells were transfected with 1.5 µg/mL of mPGES-1/pcDNA3 construct using FreeStyle Max reagent at a cell density of 1×10^6 for two days. Transfected cells were collected, washed, and sonicated in TSES buffer (15 mM Tris–HCl, pH 8.0 plus 0.25 M sucrose, 0.1 mM EDTA, and 1 mM DTT) on ice. The broken cells were first centrifuged at 12.500 × g for 10 min. The supernatant was further centrifuged at 105,000 × g for 1 h at 4 °C. The residual pellet was washed and homogenized in PBS buffer. The crude microsomal mPGES-1 was aliquoted and stored at −80 °C before use.

2.2.5.2. Activity assay using a recombinant mPGES-1. The enzyme activity assay was performed using the same protocol as described in our previous reports [59–62]. Briefly, the mPGES-1-catalyzed reaction was performed in 1.5 mL microcentrifuge tubes with reaction mixture of 0.2 Na_2HPO_4/NaH_2PO_4, pH 7.2 (10 µL); 2.5 mM GSH (2.5 µL); diluted microsomal human mPGES-1 enzyme (80 µg/mL, 1 µL); inhibitor in DMSO solution (1 µL); 0.31 mM PGH_2 in DMF (5 µL) and distilled deionized water in a final volume of 100 µL. An inhibitor was incubated with the enzyme for 15 min at ambient temperature followed by the addition of substrate PGH_2 (stored in dry ice). The enzymatic reaction was started immediately upon the addition of PGH_2. After 1 min of reaction, solution (40 mg/mL $SnCl_2$ in absolute ethanol, 10 µL) was added to cease the reaction by converting excess PGH_2 to $PGF_{2\alpha}$. The produced PGE_2 from the enzymatic reaction was quantified by the PGE_2 enzyme immunoassay as described earlier [63].

2.2.5.3. COX-1/2 enzyme activity assay. The inhibitor potential of compounds towards COX-1 and COX-2 enzymes was evaluated using a colorimetric COX Inhibitor Screening Kit (Cayman Chemical, Ann Arbor, MI, USA). The samples and control were dissolved in DMSO and diluted with reaction buffer to their final concentrations. DMSO served as a negative control for 100% initial activity. Inhibitor interference was tested by adding the inhibitor to a boiled enzyme sample as a control. The assay was conducted in duplicate.

2.2.6. Tube formation assay

Matrigel was thawed at 4 °C the night before the experiment. 48-well plates were coated with matrigel and let polymerize at 37 °C for 1 h. Cells were seeded onto the wells at a density of 250×10^3/well in culture media consisting of two different compounds (**20** and **24**) in each and incubated at regular culturing conditions for 10 h. Images for each compound well were captured under an inverted microscope and analyzed.

2.3. Molecular modeling methods

2.3.1. Preparation of the ligands

The structures of molecules were drawn and saved with mole extensions using Biovia Discovery Studio (DS) program (Dassault Systemes BIOVIA, 2017). Their geometries were optimized and prepared using the "Clean Geometry" toolkit of DS. AutoDockTool 1.5.6 (ADT) [64] was used to assign Gasteiger partial charges to each atom of the ligands in the PDB format to generate a pdbqt file. ADT interface was then used to generate grid parameter file (gpf) and a docking parameter file (dpf) to use as input files for grid mapping and docking steps.

2.3.2. Preparation of the enzyme and molecular docking calculations

The enzyme mPGES-1 used in this study (PDB ID: 5K0I, resolution: 1.30 Å) [65] was retrieved from the Protein Data Bank (https://www.rcsb.org), an online database of proteins. The protein was cleaned of water molecules, co-crystallized inhibitor, and non-interacting ions, and the missing residues inserted. All hydrogens were added, and Biovia DS 4.5 Studio was used to optimize by selecting "Clean Geometry" toolkit with a fast, Deriding-like forcefield. Further, energy minimization of the protein was carried out utilizing "Prepare Macromolecule" protocol of DS with the assignment of CHARMM force field based on the protonation state of the titratable residues at physiological pH 7.4. The enzyme COX-2 also used in this study (PDB ID: 3NT1, resolution: 1.73 Å) [66] was retrieved from the Protein Data Bank (https://www.rcsb.org), and prepared in the same way as mPGES-1. Ligands and enzyme structures were then used as input files for grid mapping and docking, respectively.

AutoDock 4.2.6 docking program (http://autodock.scripps.edu) [64] was utilized for all docking experiments. All ligands were set to be flexible, but the protein was set to be rigid. The region where 6PW ligand occupies volume during crystallization was accepted as the active site of the enzyme. The grid center coordinates of the enzyme were generated during the preparation of the gpf as 9.697, 15.296, 27.28, x, y, z respectively. Energy grid box of dimension $50 \times 50 \times 50$ Å were selected covering the entire active site of the enzyme.

Autodock 4.2′s Lamarckian Genetic Algorithm [67] with 20,000,000 energy evaluations was used for ligand conformational search. Ten independent runs were performed for each ligand, and the different conformers generated were docked randomly into the active site of these enzymes. Biovia Discovery studio visualizer program was used to render the interactions between ligands and protein complexes.

2.3.3. Molecular dynamics simulation

MD simulation was performed using NAMD software to examine the stability of the ligand binding mode of the mPGES-1 protein (http://www.ks.uiuc.edu/Research/namd/) [68]. Since the mPGES-1 is a membrane bound protein therefore it was inserted into the 1,2-palmitoyl-oleoyl–*sec* glycero–3-phosphocholine (POPC) membrane using the OPM web service (http://opm.phar.umich.edu/) [69] before preparation of the input files. CHARMM-GUI web service (http://www.Charmm.org) [70] was used for the input parameter files used in NAMD MD simulation software. The system was solvated using the TIP3P water model, water molecules were preserved and neutralized by adding 0.15 M NaCl. In the first minimization (1000 steps), the lipid tails were left mobile to induce the structure of the membrane, and other parts (lipid head groups, ion, etc.) were kept constant. After the first minimization, the system was restarted using Langevin dynamics at 310.15 K temperature. The balance of the system was achieved with a time step of 2 fs for 1 ns. In the second minimization (1000 steps) the protein backbone was limited by harmonic constraints. Water molecules were prevented from entering the hydrophobic zone of the membrane, and the system was balanced for 1 ns. With the release of harmonic constraints in the final minimization, the system is balanced more. The production run was conducted at 310.15 K and 1 atm for 50 ns without any restrictions. The stability of ligand binding modes in the system was investigated by calculating the root mean square deviation (RMSD), root mean square fluctuation (RMSF), radius of gyration (Rg). All these examinations were performed using Visual Molecular Dynamics (VMD) software.

2.4. In silico *prediction of molecular properties*

2.4.1. Determination of predicted solubility and molecular descriptors

The solubility properties and molecular descriptors of compounds 7**–30** were screened in compliance with Lipinski's Rule of 5 and Veber's rule. All synthesized thioether derivatives were controlled for their molecular weight, molecular volume, LogP, solubility, number of hydrogen bond donors/acceptors, topological polar surface area, number of rotatable bonds,%ABS, etc. All aforementioned data were obtained from online web server SwissADME [71] except volume values which were calculated by using online web server Molinspiration (http://www.molinspiration.com/cgi-bin/properties).

2.4.2. ADMET and drug-likeness profile

ADMET parameters and drug-likeness profile of the active compounds **9**–**11, 20, 21, 23, 24**, were screened according to *in vitro* assays. ADMET profile that Caco-2 permeability and P-glycoprotein substrate (absorption); BBB and CNS permeability (distribution); CYP450 enzyme inhibition (metabolism); total Clearance (excretion); mutagenic, tumorigenic, reproductive, and irritant effect with AMES (toxicity) and drug-likeness properties of selected active compounds were evaluated by using online web server pkCSM [72] and OSIRIS Datawarrior software [73] besides SwissADME .

3. Results and discussion

3.1. Synthesis and characterization of compounds

The synthesis of compounds **7–30** is outlined in Scheme 1. The compounds were synthesized starting with carvacrol etherification. Ethyl-2-[2-methyl-5-(propane-2-*yl*)phenoxy]acetate **1** obtained from the reaction of carvacrol and ethyl 2-bromoacetate as reported earlier [47,56]. Heating compound **1** with hydrazine hydrate in ethanol afforded 2-[2-methyl-5-(propane-2-*yl*)phenoxy]acetohydrazide **2**. Adding this hydrazide derivative to ethyl or methyl isothiocyanate, corresponding thiosemicarbazides **3** and **4** were obtained. [47]. 4-Ethyl/methyl-5-{[2-methyl-5-(propane-2-yl)phenoxy]methyl}−2,4-dihydro-*3H*-1,2,4-triazole-3-thione derivatives (**5, 6**) were obtained by base catalyzed cyclization of **3** and **4** in the presence of 2 N NaOH [47]. Synthesis of 2-{[3-[1-[5-methyl-2-(propane-2-yl)phenoxy]ethyl]−4-substituted-4,5-dihydro-1,2,4-triazole]sulfanyl}−1-(substituted phenyl)ethanone derivatives (**7–18**) were carried out by the reaction of appropriate bromoacetophenone derivatives and 1,2,4-triazoles (**5,6**) [57]. As the final step of the synthesis, ethanone derivatives **7–18** were reacted with hydroxylamine hydrochloride in presence of pyridine to obtain triazole-ethanone oxime conjugates **19–30** [57].

The structure of synthesized compounds were characterized by HPLC, IR, ^{1}H NMR. All ethanone derivatives **7–18** and oximes **19–30** were also characterized by LC-MS spectral data to confirm correct molecular ion peaks corresponding to $(M+H)^+$ in positive ionization and $(M\text{-}H)^-$ in negative ionization mode in each compound. For compounds **12, 14, 15, 26,** and **27** ^{13}C NMR spectra were recorded. HMBC data was also recorded for compounds **6, 7, 8, 16, 19, 23**, and **28**.

The N–H and -C=N- stretching bands of the triazole compounds **5** and **6** at 3157–3055 cm^1 and 1615–1614 cm^{-1} were consistent with the literature [36,47,74]. 1,2,4-Triazole-3-thiones might have also existed in thiol form due to the tautomerization. Compounds **5** and **6** showed C=S stretching bands at 1276 cm^{-1} and 1277 cm^{-1} respectively. These values indicated that the compounds exist in thione form, rather than thiol form [36,-74]. The absence of S-H stretching bands in the region 2600–2550 cm^{-1} is another evidence of formationf the thione form [75]. ^{1}H NMR data of these compounds also supported the occurrence of thione form and the N–H protons of 1,2,4-triazole-3-thione were observed at 13.85 ppm and 13.87 ppm whereas S-H proton was not identified [76]. In ^{13}C NMR spectra of compound **6,** C_5 carbon of the triazole ring appeared at 152.11 ppm while the thiocarbonyl carbon was detected at 167.57 ppm in accordance with the literature [36,38,47].

Compounds **7–18** showed C=O stretching bands between 1686 and 1658 cm^{-1} and the –C–S–C– absorption bands were detected at 692–678 cm^{-1}. Lack of C=S and N–H bands also proved the framework of the compounds. –S–CH_2– protons ofethanone derivatives **7–18**,resonated in the region 4.86–4.99 ppm whereas –S–CH_2– protons resonated at 5.27 ppm for all compounds. ^{13}C NMR spectra of represented compounds **7, 8, 12, 14,** and **15**, depict the signal of carbonyl carbons in the region 192.09–193.71 ppm. -S-CH_2- carbons appeared at 40.81–40.95 ppm range. The C_5 and C_2 carbons of the triazole ring were identified in the region 152.11–152.75 ppm and 150.17–150.94 ppm, respectively.

Formation of oxime structure was confirmed by the lack of C=O bands in relevant region. and, observing O–H and C=N stretching bands at 3180–3099 cm^{-1} and 1616–1606 cm^{-1} respectively. In the ^{1}H NMR spectra of oxime derivatives, O–H protons observed at 11.60–12.14 ppm indicates the formation of oxime. -S-CH_2- protons resonated downfield area (4.37–4.48 ppm) compared to the corresponding ketones due to shielding effect of the newly added OH group and diamagnetic anisotropic effect of N atom, ^{13}C NMR spectra showed conversion of the ketone C=O (192.09–193.51 ppm) to the oxime C=N (151.18–152.62 ppm). In the ESI-mass spectra of these compounds, *m/z* 276 peaks of compounds **19–24** and *m/z* 290 peaks in compounds **25–30** were observed in negative ion spectra. These peaks occur due to fragmentation of the structure via the thioether bond and removal of hydrogen.

3.2. Biological activity studies

3.2.1. Inhibition of mPGES-1 enzyme and COX-1/2 enzymes

Compounds **5–30** were screened for their inhibitory activity towards mPGES-1. Compound **4b** [5-{[3–chloro-4-(4-

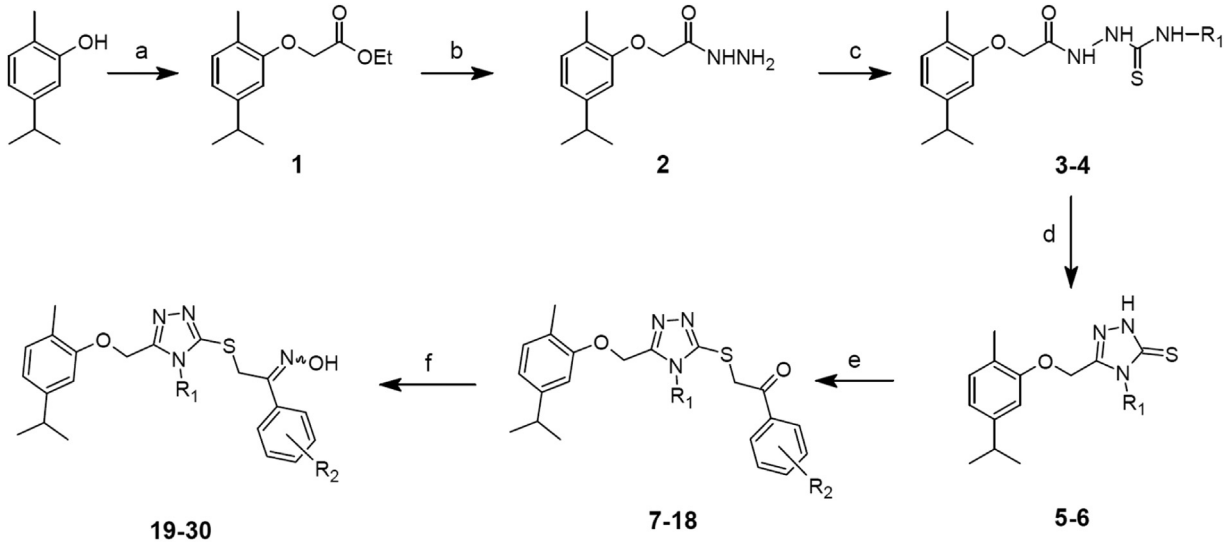

3:R_1: CH_3
4:R_1: C_2H_5
5:R_1: CH_3
6:R_1: C_2H_5

7 and **19**: R_1: CH_3, R_2: H
8 and **20**: R_1: CH_3, R_2: 4-Cl
9 and **21**: R_1: CH_3, R_2: 3,4-Cl_2
10 and **22**: R_1: CH_3, R_2: 4-F
11 and **23**: R_1: CH_3, R_2: 4-OCH_3
12 and **24**: R_1: CH_3, R_2: 4-Br

13 and **25**: R_1: C_2H_5, R_2: H
14 and **26**: R_1: C_2H_5, R_2: 4-Cl
15 and **27**: R_1: C_2H_5, R_2: 3,4-Cl_2
16 and **28**: R_1: C_2H_5, R_2: 4-F
17 and **29**: R_1: C_2H_5, R_2: 4-OCH_3
18 and **30**: R_1: C_2H_5, R_2: 4-Br

Scheme 1. Synthetic route to compounds 1–30. Key to reagents: **a.** $BrCH_2COOC_2H_5$, K_2CO_3, acetone; **b.** $NH_2NH_2.H_2O$, EtOH; **c.** R_1NCS, EtOH; **d.** 2 N NaOH,%10 HCl; **e.** TEA, acetonitrile, substituted acetophenone derivatives, **f:** $NH_2OH.HCl$, pyridine/EtOH.

cyclohexylbutoxy)phenyl]methylidene}−1,3-diazinane-2,4,6-trione] is a potent mPGES-1 inhibitor developed by the Zhan's Lab [−59] and was used as reference compound. MK-886 is also another well-recognized inhibitor used for the comparison of IC_{50} values. IC_{50} values of MK-886 and reference compound **4b** were found as 2.58±0.48 and 0.034±0.014 μM, respectively. The results are presented in Table 1. In the first line screening, compounds that caused an inhibition greater than 70% were further screened at a concentration of 10 μM. IC_{50} values were determined for the compounds that showed ≥70% inhibition at 10 μM. Among compounds **5–30**, the most potent derivative was **20** with an inhibitory concentration of 0.224±0.070 μM. Compounds **5** and **6** showed no inhibition or marginal effect on mPGES-1. This confirms the importance of phenacyl moiety via thioether linkage. On the other hand, first line results for compounds **13–18** and **25–30** revealed the unfavorable effect of ethyl group at R_1 position as none of the compounds from these series exhibited significant activity. This might be related to moieties bulkier than methyl group are not tolerated at the binding site.. mPGES-1 inhibitory activity has been observed to be increased when ketones **7–12** were converted into their oxime derivatives **19–24**, except for compounds **10** and **22** which had fluorine substitution at R_2 position. In most cases, oxime derivatives showed better inhibition compared to their ketone precursors. As a next step for the selected compounds which showed promising inhibitory activity against mPGES-1 greater than 70%, COX-1 and COX-2 inhibition profiles were also screened. Compounds 9–11, 20, 21, 23 and 24 were screened for their potential inhibition and the results are given in Table 1. All tested compounds displayed %inhibition between 52 and 67 for COX-1 and 84–86inhibition of COX-2 at 100 μM concentration. COX-1 inhibitory potential of all tested compounds was remarkably lower at the same concentration.

3.2.2. Measurement of angiogenesis by the tube formation assay

Angiogenesis involves the three main processes known as proliferation, migration, and tube-like structure formation of endothelial cells [77]. As it is known, PGE_2 promotes migration, vascular sprouting, and tube formation, enhances endothelial survival, and directly stimulate the synthesis of proangiogenic factors [78]. The three different experimental approaches can be used namely *in vitro* tube formation, *in vivo* chicken chorioallantoic membrane (CAM) blood vessel formation, and *ex vivo* mouse thoracic aorta ring outgrowth to probe angiogenic effects of PGE_2 [30]. Tube formation assay is one of the most used *in vitro* assays to determine the extent of angiogenesis. The assay is based on the ability of endothelial cells to form a three-dimensional capillary like structure and measures the ability of compounds to promote or inhibit the formation of these tubes [79]. Due to the reported relationship between inhibition or deletion of mPGES-1 enzyme responsible for PGE_2 production and angiogenesis [34,80], Matrigel tube formation assay was performed to understand the anti-angiogenic properties of compounds **20** and **24**. As shown in Fig. 2, compounds **20** and **24** significantly prevented the tube formation.

To reveal the mechanism under this prevention, the viability of HUVEC cells was measured in a dose dependent manner (5 nM-10 μM). No significant difference was observed between cell viability values for treated and untreated cells at all dose values. These results indicated that compounds **20** and **24** did not effect on cell viability. (Fig. 3).

3.2.3. Cytotoxic activity of the synthesized compounds

Compounds **5–30** were screened for their antiproliferative activity against MCF-7, A549, PC-3, HeLa, K562, and NIH/3T3 cells. MTT assay was used for this study. The results of initial screening data at 10 μM were summarized in Table S1 (see supplementary material). The compounds which have an inhibitory effect greater than 30%, were selected for the determination of IC_{50} values in respective cell lines (Table 2). Compound **15** exhibited anticancer activity with an IC_{50} value of 23.77 μM against HeLa cell line while compound **18** showed activity against A549 cell line at 16.28 μM. These compounds were also chosen for apoptotic pathway studies. Unlike the results of mPGES-1 enzyme inhibition data, none of the com-

Table 1
Inhibition profile of compounds **5–30** against mPGES-1 and COX-1/2.

Compound	R_1	R_2	Lab ID Code	mPGES-1% Inhibition at 10 μM[a]	mPGES-1 IC_{50} (μM, Mean±SD)[b]	% Inhibition of	
						COX-1 (at 100 μM)	COX-2 (at 100 μM)
5	CH_3	–	KUC16GE1	0	–	–	–
6	C_2H_5	–	KUC16GE2	21±9.5	–	–	–
7	CH_3	H	KUC16F061	22±0.1	–	–	–
8	CH_3	4-Cl	KUC16F064	16±8.4	–	–	–
9	CH_3	3,4-Cl_2	KUC16F066	**73±8.6**	**3.83±1.66**	62.94	85.77
10	CH_3	4-F	KUC16F069	**69±12**	**3.051±1.10**	63.12	85.20
11	CH_3	4–OCH_3	KUC16F071	**84±8.5**	**1.46±0.44**	57.09	86.27
12	CH_3	4-Br	KUC16F075	0	–	–	–
13	C_2H_5	H	KUC16F081	2.0 ± 6.5	–	–	–
14	C_2H_5	4-Cl	KUC16F084	0	–	–	–
15	C_2H_5	3,4-Cl_2	KUC16F086	30±2.7	–	–	–
16	C_2H_5	4-F	KUC16F089	14±13	–	–	–
17	C_2H_5	4–OCH_3	KUC16F091	22±9.0	–	–	–
18	C_2H_5	4-Br	KUC16F095	53±9.1	–	–	–
19	CH_3	H	KUC16G061	55±20	–	–	–
20	CH_3	4-Cl	KUC16G064	**83±3.5**	**0.224±0.070**	67.73	85.96
21	CH_3	3,4-Cl_2	KUC16G066	**97±7.1**	**1.54±0.28**	66.67	84.39
22	CH_3	4-F	KUC16G069	0	–	–	–
23	CH_3	4–OCH_3	KUC16G071	**88±17**	**2.44±0.98**	66.31	84.76
24	CH_3	4-Br	KUC16G075	**85±9.4**	**1.08±0.35**	52.13	85.89
25	C_2H_5	H	KUC16G081	6.5 ± 8.6	–	–	–
26	C_2H_5	4-Cl	KUC16G084	50±30	–	–	–
27	C_2H_5	3,4-Cl_2	KUC16G086	35±3.3	–	–	–
28	C_2H_5	4-F	KUC16G089	32±13	–	–	–
29	C_2H_5	4–OCH_3	KUC16G091	0	–	–	–
30	C_2H_5	4-Br	KUC16G095	22±14	–	–	–
MK-886 [c]				2.58±0.48	–	–	–
4b [c]				0.034±0.014	–	–	–

[a] Data are expressed as means ± SD of single determinations obtained in triplicate.
[b] IC_{50} values were determined only for the compounds that showed ≥70% inhibition at 10 μM. Data are expressed as means ± SD of single determinations obtained in triplicate.
[c] Compounds MK-886 and compound **4b** were used as reference compounds for the determination of IC_{50} values. MK-886 is a well-recognized inhibitor against mPGES-1 and reference compound **4b** is the inhibitor developed by Chang Guo Zhan's lab.

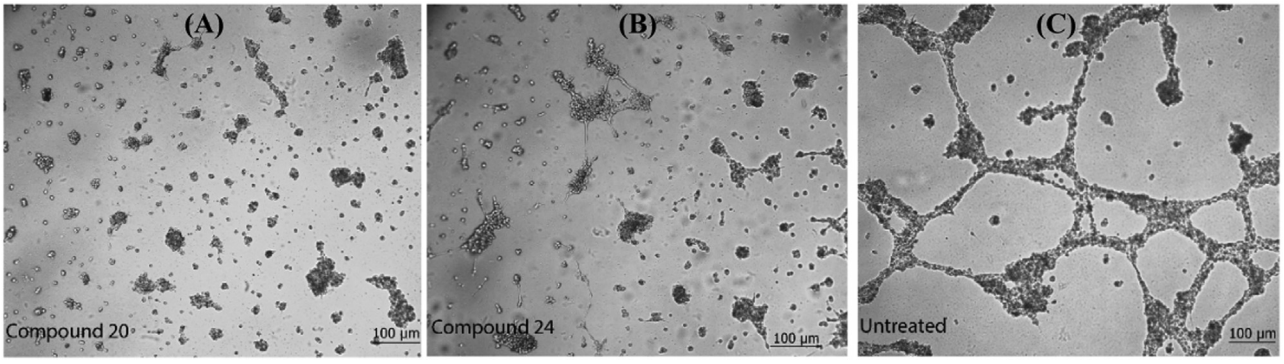

Fig. 2. Inhibition of tube formation by mPGES-1 inhibitors **20** and **24** in HUVEC cells. (A) cells treated with compound **20**; (B) cells treated with compound **24**; (C) untreated cells.

Table 2
In vitro cytotoxic effects of selected compounds against human cancer cell lines and mouse embryonic fibroblast cells.

Compound Code	IC_{50} (μM)			
	A549	PC-3	HeLa	NIH/3T3
9	42.25	–	–	74.66
10	–	47.65	–	86.59
11	76.86	–	–	69.88
12	95.35	–	–	33.25
14	–	–	57.89	61.55
15	36.83	–	23.77	55.83
16	40.16	–	–	86.35
17	38.32	–	92.89	42.30
18	16.28	–	–	66.12
Imatinib	53.61	25.48	29.37	>300

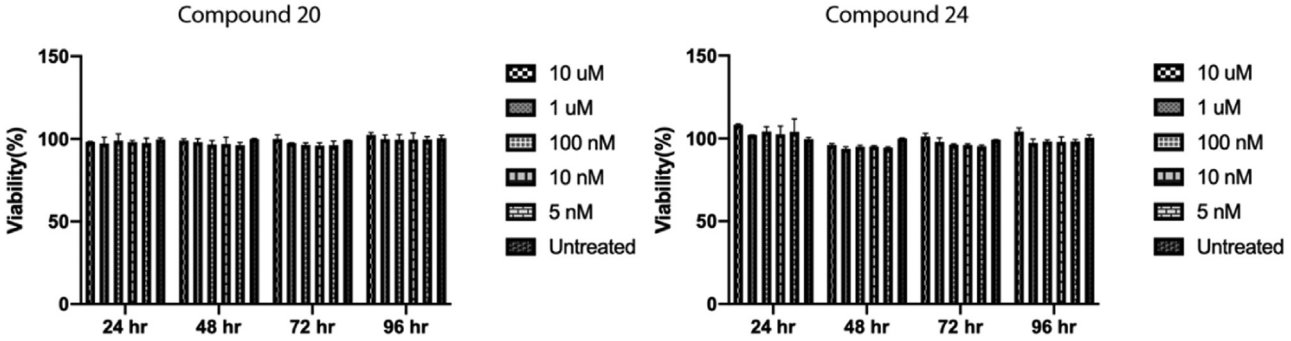

Fig. 3. Cytotoxicity testing of compounds **20** and **24** on HUVEC cells.

Table 3
Binding energy values of all synthesized compounds for mPGES-1 and COX-2.

Compound	Ketone derivatives	Binding energy (kcal/mol)		Compound	Oxime derivatives	Binding energy (kcal/mol)	
	Lab ID Code	mPGES-1	COX-2		Lab ID Code	mPGES-1	COX-2
MK886	–	−6.19	−5.17				
7	KUC16F061	−6.64	−5.59	19	KUC16G061	−6.46	−5.61
8	KUC16F064	−6.56	−5.69	20	KUC16G064	−7.12	−5.45
9	KUC16F066	−6.87	−6.12	21	KUC16G066	−7.54	−5.95
10	KUC16F069	−6.49	−5.64	22	KUC16G069	−6.28	−5.30
11	KUC16F071	−6.13	−5.44	23	KUC16G071	−6.59	−6.29
12	KUC16F075	−7.06	−5.70	24	KUC16G075	−7.4	−5.88
13	KUC16F081	−6.32	−5.48	25	KUC16G081	−6.37	−4.97
14	KUC16F084	−6.78	−6.02	26	KUC16G084	−6.23	−5.70
15	KUC16F086	−6.95	−5.66	27	KUC16G086	−6.6	−5.60
16	KUC16F089	−6.31	−5.29	28	KUC16G089	−6.66	−5.39
17	KUC16F091	−6.77	−5.67	29	KUC16G091	−6.87	−5.35
18	KUC16F095	−6.85	−5.74	30	KUC16G095	−6.73	−5.95

Table 4
Types of interactions of the inhibitors and MK-886 with the binding site residues of mPGES-1 enzyme.

Compound	Lab ID Code	Number of H-bonds	Distance of H-bonds (Å)	H-bonds interactions	Hydrophobic interactions
MK886	–	1	1.88	TYR130: H (COOH)	THR130 (pi-pi stacking)
9	KUC16F066	3	3.06	ASN74: Cl	THR130 (pi-pi stacking)
			2.54	THR131: O (C=O)	
			3.29	THR131: Triazole (N)	
10	KUC16F069	4	2.81	THR131: O (C=O)	TYR130 (pi-pi stacking)
			2.96	ASN74: F	
			2.99	SER137: Triazole (N2)	HIS113(halogen:fluorine)
			2.82	ARG126: Triazole (N3)	
11	KUC16F071	2	2.94	THR131: O (C=O)	TYR130 (pi-pi stacking)
			2.89	THR131: Triazole (N)	GLN134 (pi-pi stacking)
					ARG126 (pi-cation)
20	KUC16G064	4	2.69	ARG126: Carvacrol-O	TYR130 (pi-pi stacking)
			2.69	ASN74: Triazole (N2)	
			2.77	ARG73: Triazole (N3)	
			2.24	GLU77: H (N–O-H)	
21	KUC16G066	3	3.60	TYR130: S	ARG126 (pi-cation)
			3.22	ARG73: Cl	TYR130 (pi-pi stacking)
			1.73	GLU77: H (N–O-H)	ARG73 (pi-anion)
					GLU77 (pi-anion)
23	KUC16G071	4	2.87	SER127: Carvacrol-O	ARG126 (pi-cation)
			2.75	TYR130: N (N–O-H)	
			2.00	GLU77: H (N–O-H)	TYR130 (pi-pi stacking)
			2.70	ARG73: O (OCH3)	
24	KUC16G075	3	3.28	ARG126: Carvacrol-O	TYR130 (pi-pi stacking)
			2.29	SER127: H (N–O-H)	
			1.97	THR131: H (N–O-H)	

pounds carrying oxime group showed significant activity as well as the compounds carrying methyl substituent at the 4th position of the triazole ring. No significant cell inhibitory effect was observed in DMSO treated samples. The compounds were also tested for cytotoxic effects in NIH-3T3. According to cytotoxicity results, the selectivity index of compound **18** was determined as 4 for A549 cell line (NIH3T3-IC_{50} / A549-IC_{50}).

3.2.4. Apoptosis

Compound **15** caused reduction in MMP and triggered apoptosis, especially through the mitochondrial internal pathway where caspase-9 was active. As caspase-8 activity did not differ compared to control, it was concluded that compound **15** induced caspase-9-mediated apoptosis and increased caspase-3 activity.

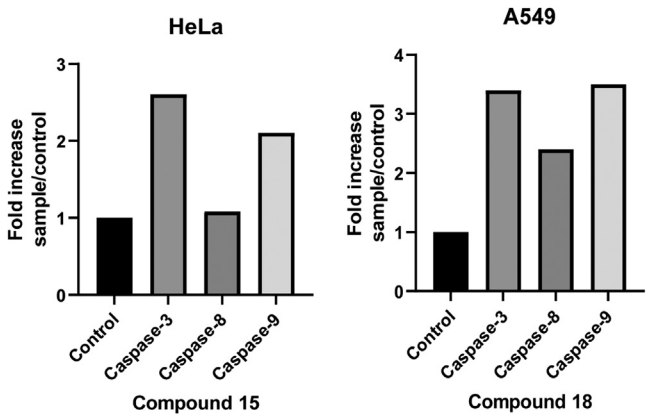

Fig. 4. Caspase activities of compounds **15** and **18**.

On the other hand, the effect of compound **18** on A549 cells was found to be occurred by both internal and external pathways of apoptosis. It was found that caspase-9 activity increased due to disruption of MMP and activated caspase-9 stimulated activation

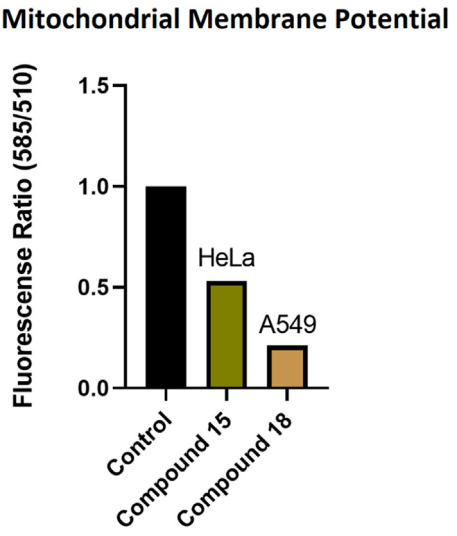

Fig. 5. Mitochondrial membrane potential changes for compounds **15** and **18**.

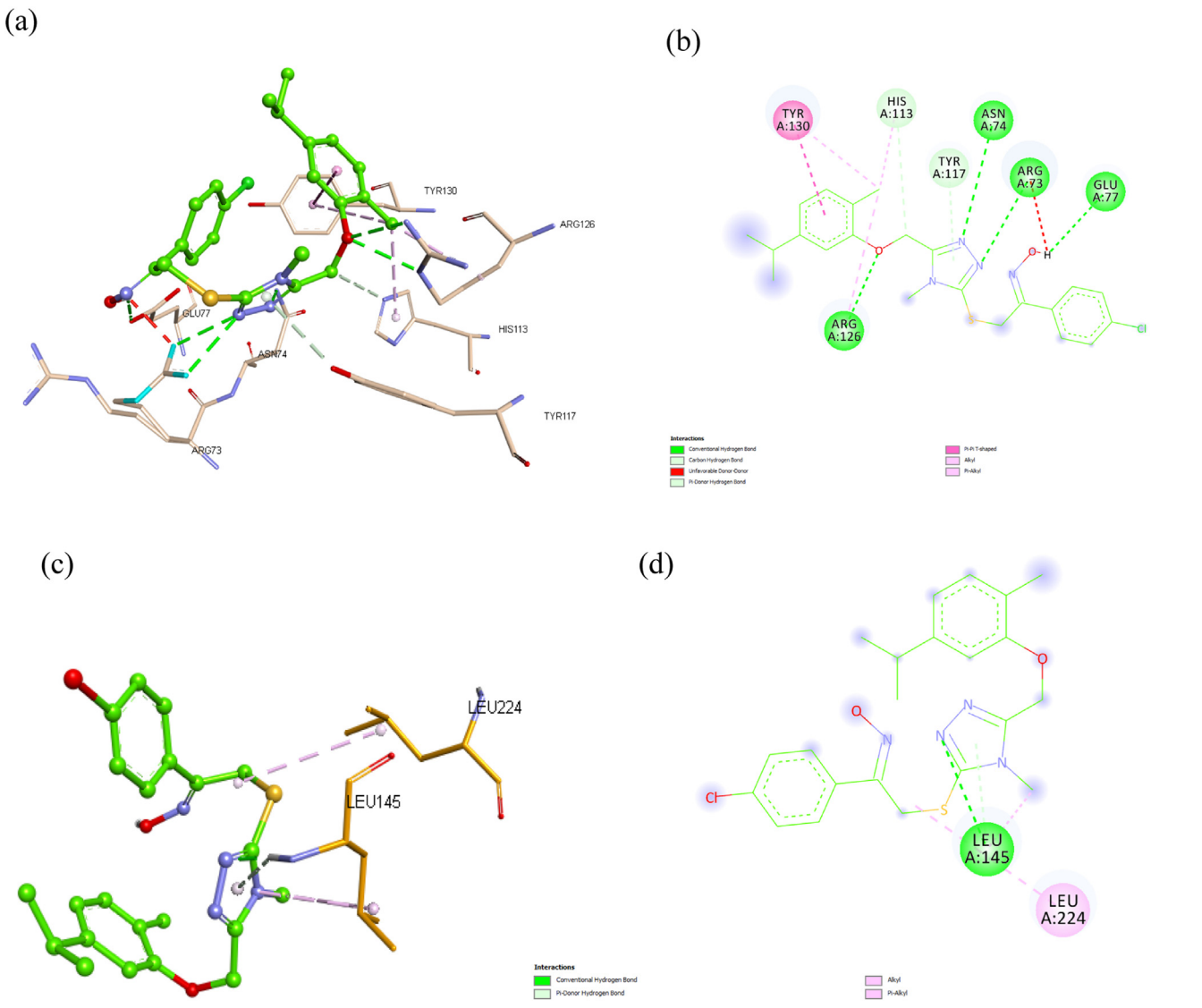

Fig. 6. Binding mode compound **20** to mPGES-1 in the 3D space (a); and the corresponding interaction diagram shown in the 2D scheme (b); to COX-2 in the 3D space (c); and the corresponding interaction diagram shown in the 2D scheme (d).

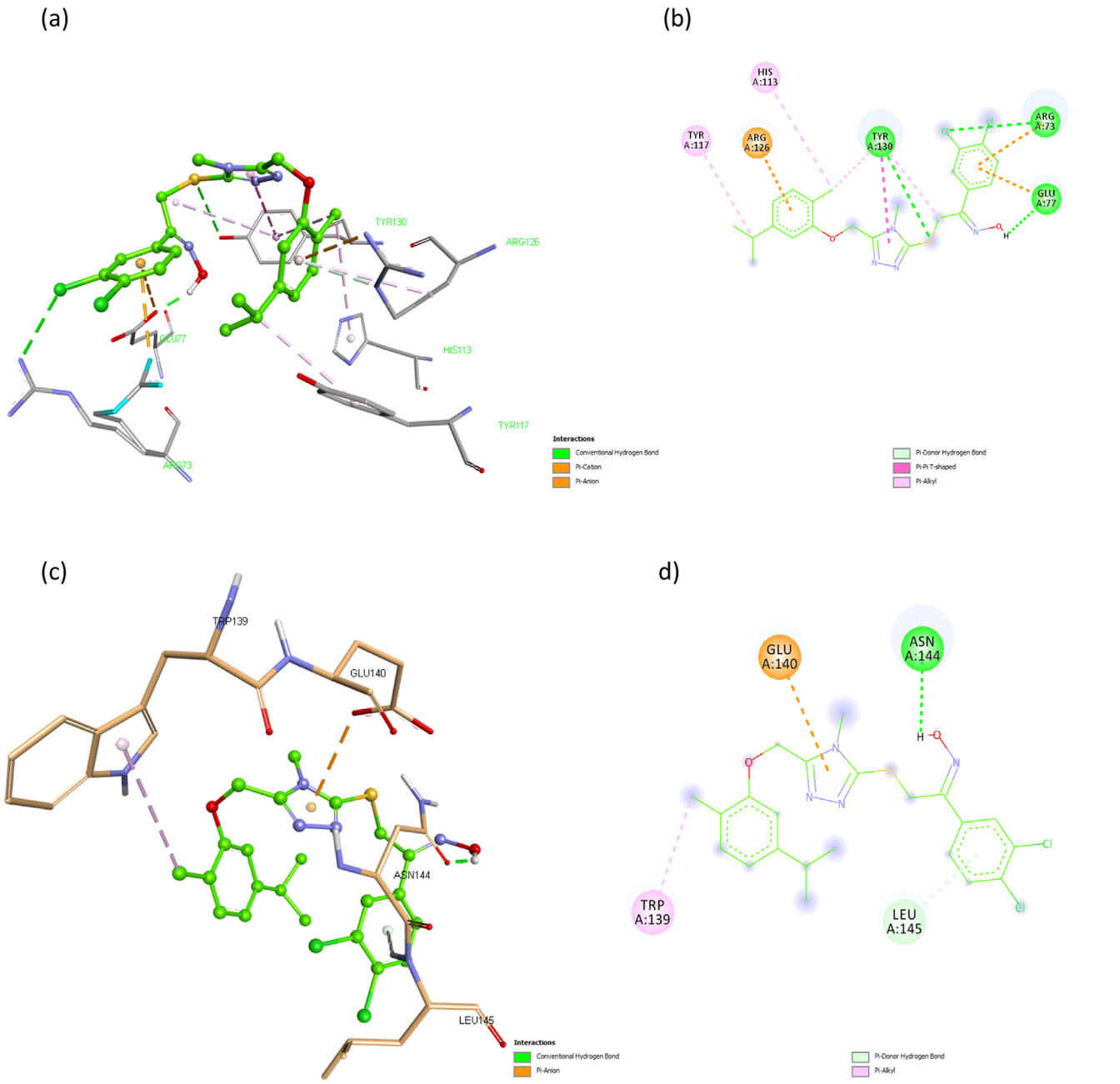

Fig. 7. Binding mode of compound **21** to mPGES-1 in the 3D space (a); and the corresponding interaction diagram shown in the 2D scheme (b); to COX-2 in the 3D space (c); and the corresponding interaction diagram shown in the 2D scheme (d).

of caspase-3, the terminating molecule of the apoptotic pathway. Unlike compound **15**, compound **18** caused an increase in caspase-8 activity (Figs. 4 and 5).

3.3. In silico *studies*

3.3.1. *Molecular docking and conformation analysis*

Although mPGES-1 enzyme exists as a homotrimer, only one monomer is active at a time in the open conformation of the enzyme which was used for modeling studies. mPGES-1 catalyzes the isomerization of PGH_2 to PGE_2 and glutathione (GSH) is an essential cofactor for its catalytic turnover. GSH is bound within the active site in a U-shaped conformation via hydrogen bonds (ARG 38, ARG73, ASN74, GLU77, HIS113, TYR117, ARG126, and SER127), pi-pi stacking (TYR130) interactions as well as other hydrophobic and polar interactions. The experimental results indicated that in a structure-based design, a potential inhibitor can act as a false substrate (PGH_2) and a cofactor analog (GSH). Thus, the U-shape conformation of ligands in the active site is important for the inhibition of this enzyme. Most of the known mPGES-1 inhibitors bind to the substrate and glutathione (GSH) cofactor binding sites simultaneously [81]. Therefore, the substrate and cofactor binding pockets volume were utilized for the docking studies.

The computational binding energies of compounds for mPGES-1 and COX-2 enzymes are presented in Table 3. The computational binding energies of compounds **7–19** were slightly lower than that of experimental values. On the other hand, all compounds showed better binding values against mPGES-1, compared to COX-2 enzyme. MK-886 was used as a reference compound. Compounds **20,**

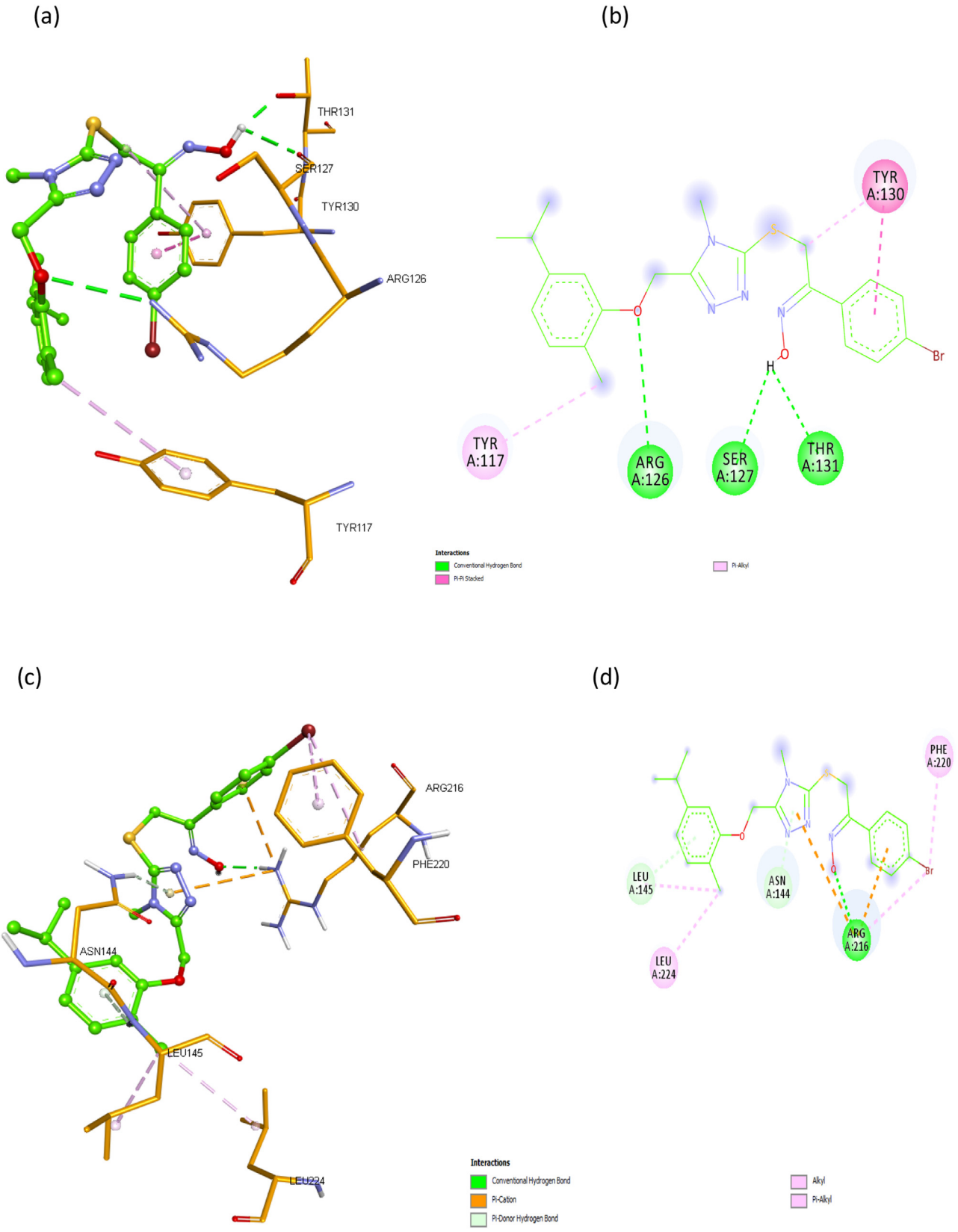

Fig. 8. Binding mode of compound **24** to mPGES-1 in the 3D space (a); and the corresponding interaction diagram shown in the 2D scheme (b); to COX-2 in the 3D space (c); and the corresponding interaction diagram shown in the 2D scheme (d).

Table 5
Solubility and molecular descriptors of compounds **7**–**30** from SwissADME.

Compound	MW (g/mol)	$LogP_{o/w}$	LogS (ESOL)	nON	nOHN	nRot	TPSA	%ABS	Lipinski Rule nviol	Veber's Rule nviol
7	395.52	4.14	−5.16	4	0	8	82.31	79.60	–	–
8	429.96	4.61	−5.75	4	0	8	82.31	79.60	–	–
9	464.41	5.21	−6.35	4	0	8	82.31	79.60	–	–
10	413.51	4.42	−5.31	5	0	8	82.31	79.60	–	–
11	425.54	4.15	−5.23	5	0	9	91.54	77.42	–	–
12	474.41	4.76	−6.06	4	0	8	82.31	79.60	–	–
13	409.54	4.47	−5.35	4	0	9	82.31	79.60	–	–
14	443.99	4.97	−5.95	4	0	9	82.31	79.60	–	–
15	478.43	5.52	−6.54	4	0	9	82.31	79.60	–	–
16	427.53	4.78	−5.51	5	0	9	82.31	79.60	–	–
17	439.57	4.42	−5.43	5	0	10	91.54	77.42	–	–
18	488.44	5.08	−6.27	4	0	9	82.31	79.60	–	–
19	410.53	4.06	−5.40	5	1	8	97.83	75.25	–	–
20	444.98	4.67	−5.99	5	1	8	97.83	75.25	–	–
21	479.42	5.20	−6.59	5	1	8	97.83	75.25	–	–
22	428.52	4.43	−5.56	6	1	8	97.83	75.25	–	–
23	440.56	4.11	−5.47	6	1	9	107.06	72.06	–	–
24	489.43	4.74	−6.31	5	1	8	97.83	75.25	–	–
25	424.56	4.38	−5.59	5	1	9	97.83	75.25	–	–
26	459.00	4.90	−6.19	5	1	9	97.83	75.25	–	–
27	493.45	5.51	−6.79	5	1	9	97.83	75.25	–	–
28	442.55	4.75	−5.75	6	1	9	97.83	75.25	–	–
29	454.59	4.33	−5.67	6	1	10	107.06	72.06	–	–
30	503.46	4.98	−6.50	5	1	9	97.83	75.25	–	–

MW: Molecular weight; LogP o/w: Consensus; LogS (ESOL): Estimating aqueous solubility from molecular structure; nON: Number of hydrogen acceptors; nOHN: Number of hydrogen donors; nRot: Number of rotatable bonds; TPSA: Topological polar surface area;%ABS: Percentage of absorption.

Table 6
Predicted ADMET properties and drug-likeness of **9–11, 20, 21, 23** and **24**.

ADMET Properties		9	10	11	20	21	23	24
Absorption	Caco2 permeability (10^{-6} cm/s)[a]	High	High	High	High	High	High	High
	% Human intestinal absorbtion[a]	High	High	High	High	High	High	High
	P-glycoprotein substrate[b]	No	No	No	No	No	No	No
Distribution	BBB permeability[b]	No	No	No	No	No	No	No
	CNS permeability[a]	Yes	No	No	No	Yes	No	No
Metabolism	CYP1A2 inhibitior[b]	No	No	No	No	No	No	No
	CYP2C19 inhibitior[b]	Yes	Yes	Yes	Yes	Yes	Yes	Yes
	CYP2C9 inhibitior[b]	Yes	Yes	Yes	Yes	Yes	Yes	Yes
	CYP2D6 inhibitior[b]	No	Yes	No	No	No	No	No
	CYP3A4 inhibitior[b]	Yes	Yes	Yes	Yes	Yes	Yes	Yes
Excretion	Total Clearance[a] (log ml/min/kg)	0.068	−0.129	0.053	0.031	0.159	0.081	0.01
Toxicity	AMES toxicity[a]	No	No	No	No	No	No	No
	Mutagenic[c]	None	None	None	None	None	None	None
	Tumorigenic[c]	None	None	None	None	None	None	None
	Reproductive[c]	None	None	None	None	None	None	None
	Irritant[c]	High	High	High	High	High	High	High
Medicinal Chemistry	PAINS[b]	–	–	–	–	–	–	–
	Brenk[b]	–	–	–	3	3	3	3
	Drug-likeness[c]	3.12	1.71	3.13	2.53	2.53	2.55	0.67

[a] These studies were performed by using online webserver pkCSM (http://biosig.unimelb.edu.au/pkcsm).
[b] These studies were performed by using online webserver SwissADME (http://www.swissadme.ch).
[c] These studies were performed by using OSIRIS data warrior software (http://www.openmolecules.org/datawarrior).

21, and **24** have better binding energy values than the reference compound MK-886.

The docking poses of the compounds **9–11, 20, 21, 23, 24** and reference compound MK-886, were rendered in detail to see their interaction with the residues lining the active site of the enzyme (Table 4). As a result of molecular docking studies, it has been found remarkable that the most active compounds **20, 21,** and **24** have a U-shaped conformation in the active site and exhibit hydrogen bond interactions, like glutathione. In particular, the fact that compound **20** forms four strong hydrogen bond interactions (ARG73, ASN74, GLU77, and ARG126) besides a pi-pi stacking interaction, supports the determination of this compound as the most active inhibitor in the *in vitro* enzyme assay studies (Fig. 6a, b). Compound **21** which has the highest binding energy, exhibited three hydrogen bonds (ARG73, GLU77, TYR130) besides various strong hydrophobic interactions with the active site residues such as ARG126 (pi-cation), TYR130 (pi-pi stacking), ARG73 (pi-anion), GLU77 (pi-anion) and ARG126 (pi-cation) (Fig. 7a, b). Like compound **21**, compound **24** displayed three strong hydrogen bonds with the active site residues (THR131 1.97 Å, SER127 2.29 Å and ARG126 3.28 Å). In addition, a pi-pi stacking interaction with TYR130 indicates that compound **24** is one of the best inhibitors (Fig. 8a, b).

Hydrogen bond interactions detected with the active site of COX-2 enzyme were as follows: between triazole nitrogen of compound **20** and LEU145 (Fig. 6d); between H (=*N*–OH) atom of compound **21** and ASN144 (Fig. 7d); between O (=*N*–OH) atom of compound **24** and ARG216 (Fig. 8d). Moreover, hydrophobic interactions of all compounds with COX-2 binding site were observed weakly compared to mPGES-1. Considering both *in vitro* and *in silico* mPGES-1 enzyme inhibition results of the compounds, molecular dynamics studies of compound **20** were carried out.

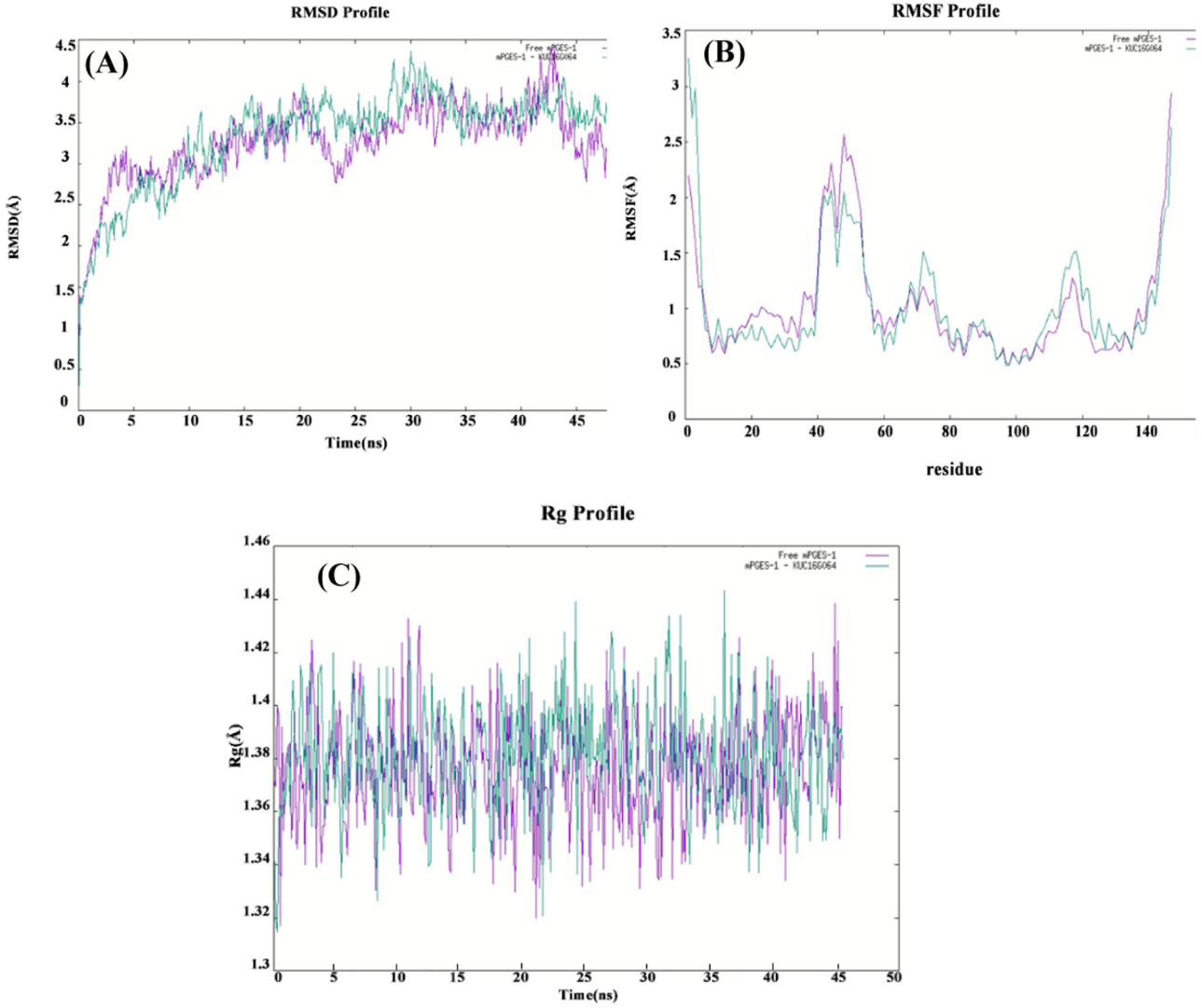

Fig. 9. RMSD (a), RMSF (b) and Rg (c) of free mPGES-1 (purple) and mPGES-1– compound **20** (green) complexes.

3.3.2. Molecular dynamics simulation analysis

To evaluate the structural stability of the simulated-docked system, (RMSD), (RMSF), and (Rg) of all orbits were analyzed. RMSD profiles show the structural stability of the protein. The RMSDs of the unbound mPGES-1 and mPGES-1-compound **20** complex were compared (Fig. 9a). Both free protein and complex RMSD values were in the range of 4.5–1.5 Å. The mPGES1-compound **20** complex showed higher stability by the end of the simulation. The RMSF profile shows residual fluctuation with time. Two residues of free mPEGS-1 showed high fluctuations of 2.7 and 3 Å, respectively (Fig. 9b). Less fluctuations of residues observed in the complex structure indicate that the complex is more stable. In other words, residues involved in the interaction with the inhibitor showed less fluctuation, proving that the complex is more stable. The (Rg) shows the compactness of the protein structure, reflecting the 3D structural stability. The Rg profile of the complex was found to be in the range of 1.3–1.45 Å, while free mPGES-1 varied between 1.3 and 1.44 Å throughout the simulation. Consequently, the Rg was found to be consistent with the RMSD and RMSF distributions for mPGES-1-compound 20. (Fig. 9c).

3.3.3. In silico admet studies

ADMET properties were calculated by using SwissADME calculation software (http://www.swissadme.ch) [71], online web server pkSCM (http://biosig.unimelb.edu.au/pkcsm) [72]. *In silico* toxicity data was evaluated by OSIRIS Data warrior software (http://www.openmolecules.org/datawarrior). SMILES codes of the compounds were generated from the structures using the ACD/ChemSketch version 12.0 molecular editor.

ADME properties were performed for LogP, LogS, number of hydrogen bond acceptors (nON) and donors (nOHN), number of rotatable bonds (nRot), topological polar surface area (TPSA), absorption (%ABS) and simple molecular descriptors used by Lipinski's rule of five and Veber (Table 5). LogP is an important value that indicating lipophilicity and according to Lipinski's rule of five, logP value should be $\leq$5. LogP value was found smaller than 5 for all screened compounds except for compounds **9, 15, 18, 21,** and **27**. LogS is estimated aqueous solubility from molecular structure and all molecules were found moderately soluble.

The number of hydrogen bond donors varied from 0 to 1 and the number of hydrogen bond acceptors varied from 4 to 6. According to Lipinski's rule of five, these values should be smaller than 5 and 10 respectively. None of the compounds violated this Lipinski rule. All the tested compounds have less than 10 rotatable bonds which indicates low conformational flexibility.

Total polar surface area (TPSA) is an important property of a molecule in transportation through biological membranes. High TPSA values give rise to poor bioavailability and absorption of a

drug. Calculated percentages of absorption for compounds **7**–**30** ranged between 82 and 107%. For compounds **11, 17, 23,** and **29** which carry –OCH_3 substituent, TPSA values were found too high. Therefore, the absorption value of these drugs was found lower than other compounds. Estimated intestinal absorption (%ABS) was calculated by:%ABS = 109 – [0.345 x topological polar surface area (TPSA)] according to the method of [82], %ABS values found between 72.06 and 79.60%.

P-glycoprotein (P-gp) is an ATP-dependent transmembrane protein and plays important role in drug absorption and penetration through blood-brain barrier (BBB). This protein can be excessively found in tumor cells and leads to drug resistance [83]. None of the selected compounds was substrate for P-gp and have no BBB permeability.

Caco-2 cell line is derived from human colon carcinoma and Caco-2 permeability assay was used to predict human intestinal permeability [84]. All tested compounds showed high Caco-2 permeability.

Even though all active compounds were found to be safe based on the *in silico* toxicity studies for AMES toxicity, mutagenicity, tumorigenicity, and reproductive effects, these active compounds have been observed to have a potential for irritant effects (Table 6).

It is known that PAINS [85] and Brenk [86] alert data can recognize the portion in a molecule that may cause some undesirable effects *in vivo*. When lead-like properties were investigated for selected active compounds, no PAINS alert was detected. The drug-likeness value of these compounds is given in Table 6.

4. Conclusion

Novel 1,2,4-triazoles and their oxime derivatives were synthesized and characterized by appropriate spectral analysis and evaluated their biological applications. Compounds **9**–**11, 20, 21, 23,** and **24**, prominently inhibited (>70) mPGES-1 enzyme with IC_{50} values between 0.224±0.070 and 3.83±1.66 µM in contrast to the reference compound MK-886 (2.58±0.48 µM). Compounds carrying oxime group (**20, 21, 23, 24**) showed better activity compared to the thioether derivatives (**9–11).** None of the compounds carrying ethyl substituent at 4th position of the triazole ring (**13–18** and **25–30**) showed inhibition greater than 50%. The structure-activity relationships pointed, methyl substitution at the fourth position of the 1,2,4-triazole ring seems to be important for mPGES-1 inhibition. Among all compounds, compound **20** carrying methyl substituent on triazole ring and oxime group showed significant inhibitory activity against mPGES-1 at 0.224±0.070 µM. Molecular dynamics studies of compound **20** supported that this compound could be a potential inhibitor for mPGES-1 enzyme.

Since both mPGES-1 and COX-2 enzymes have a significant role in PGE_2 biosynthesis, compounds **9–11, 20, 21, 23,** and **24** were also screened for their inhibitory activity towards COX-1 and COX-2 to investigate their selectivity. At 100 µM concentration, all tested compounds showed inhibitory activity greater than 80% against COX-2. These data indicated that compounds may also have an inhibitory effect against COX-2.

Due to the side effects reported with angiogenesis inhibitors targeting VEGF, less cytotoxic novel agents are needed. Compounds **20** and **24** significantly prevented tube formation without any toxicity on the HUVEC cells. Therefore, these compounds can be considered as new candidates for angiogenesis inhibitors.

For compounds **5–30**, cytotoxicity assays were also evaluated against MCF-7, A549, PC-3, HeLa, K562 and NIH/3T3 cell lines. Among them, compound **15** showed inhibition at 23.77 µM against HeLa and compound **18** showed activity against A549 cell line at 16.28 µM. Compound **15** also induced apoptosis by increasing caspase-3 activity as well as compound **18**. Compound **18** also increased caspase-8 activity. Both compounds reduced mitochondrial membrane potential.

Although molecular modeling studies of **20** and **24** compounds agreed well with the experimental results, interactions of **20** were found stronger than that of **24**. Molecular dynamics studies of compound **20** also generated additional support indicating that this compound was the best inhibitor for mPGES-1, as in experimental results. Concerning *in silico* ADMET and drug similarity studies, the active compounds **9–11, 20, 21, 23,** and **24** which have been predicted to show high Caco-2 permeability and human intestinal absorption, are not P-gp substrates. For the most active compound **20** which has no BBB and CNS permeability, any violation of Lipinski's and Veber's rules has not been observed. Finally, compound **20** was found to be safe except for its high irritant effect, based on the *in silico* toxicity studies.

Declaration of Competing Interest

The authors declare that they have no known competing financial interests or personal relationships that could have appeared to influence the work reported in this paper.

Data Availability

The authors are unable or have chosen not to specify which data has been used.

CRediT authorship contribution statement

Gizem Erensoy: Investigation, Methodology, Formal analysis, Visualization, Validation, Writing – original draft, Writing – review & editing. **Kai Ding:** Investigation, Formal analysis, Visualization, Writing – original draft, Writing – review & editing. **Chang-Guo Zhan:** Investigation, Methodology, Writing – original draft, Writing – review & editing. **Gamze Çiftçi:** Investigation, Software, Formal analysis, Validation, Visualization, Writing – original draft, Writing – review & editing. **Kemal Yelekçi:** Investigation, Software, Methodology, Writing – original draft, Writing – review & editing. **Merve Duracık:** Visualization, Writing – original draft, Writing – review & editing. **Özlem Bingöl Özakpınar:** Methodology, Formal analysis, Writing – original draft, Writing – review & editing. **Esra Aydemir:** Methodology, Validation, Writing – original draft, Writing – review & editing. **Zübeyde Nur Yılmaz:** Formal analysis, Visualization, Writing – original draft, Writing – review & editing. **Fikrettin Şahin:** Supervision, Methodology, Writing – review & editing. **Necla Kulabaş:** Formal analysis, Visualization, Software, Writing – original draft, Writing – review & editing. **Esra Tatar:** Funding acquisition, Methodology, Writing – original draft, Writing – review & editing. **İlkay Küçükgüzel:** Funding acquisition, Methodology, Conceptualization, Supervision, Visualization, Writing – original draft, Writing – review & editing.

Acknowledgments

This work was supported by Marmara University Scientific Research Projects Commission under the grants with numbers of SAG-C-DRP-081117-0616 and SAG-A-070617-0336.

Supplementary materials

Supplementary material associated with this article can be found, in the online version, at doi:10.1016/j.molstruc.2022.134154.

References

[1] M. Murakami, Lipid Mediators in Life Science, Exp. Anim. 60 (2011) 7–20, doi:10.1538/expanim.60.7.

[2] B. Samuelsson, R. Morgenstern, P.-J. Jakobsson, Membrane prostaglandin E synthase-1: a novel therapeutic target, Pharmacol. Rev. 59 (2007) 207–224, doi:10.1124/pr.59.3.1.

[3] H. Akasaka, S.-P. So, K.-H. Ruan, Relationship of the Topological Distances and Activities between mPGES-1 and COX-2 *versus* COX-1: implications of the Different Post-Translational Endoplasmic Reticulum Organizations of COX-1 and COX-2, Biochemistry 54 (2015) 3707–3715, doi:10.1021/acs.biochem.5b00339.

[4] P.-J. Jakobsson, S. Thoren, R. Morgenstern, B. Samuelsson, Identification of human prostaglandin E synthase: a microsomal, glutathione-dependent, inducible enzyme, constituting a potential novel drug target, Proc. Natl. Acad. Sci. 96 (1999) 7220–7225. https://doi.org/10.1073/pnas.96.13.7220.

[5] M. Wang, W.L. Song, Y. Cheng, G.A. FitzGerald, Microsomal prostaglandin E synthase-1 inhibition in cardiovascular inflammatory disease, J. Intern. Med. 263 (2008) 500–505, doi:10.1111/j.1365-2796.2008.01938.x.

[6] K. Larsson, P.J. Jakobsson, Inhibition of microsomal prostaglandin E synthase-1 as targeted therapy in cancer treatment, Prostaglandins Other Lipid Mediat 120 (2015) 161–165, doi:10.1016/j.prostaglandins.2015.06.002.

[7] B. Bülbül, İ. Küçükgüzel, Microsomal Prostaglandin E2 Synthase-1 as a New Macromolecular Drug Target in the Prevention of Inflammation and Cancer, Anticancer Agents Med. Chem. 19 (2019) 1205–1222, doi:10.2174/1871520619666190227174137.

[8] Y. Jin, C.L. Smith, L. Hu, K.M. Campanale, R. Stoltz, L.G. Huffman, T.A. McNearney, X.Y. Yang, B.L. Ackermann, R. Dean, A. Regev, W. Landschulz, Pharmacodynamic comparison of LY3023703, a novel microsomal prostaglandin E Synthase 1 inhibitor, with celecoxib, Clin. Pharmacol. Ther. 99 (2016) 274–284, doi:10.1002/cpt.260.

[9] Y. Jin, A. Regev, J. Kam, K. Phipps, C. Smith, J. Henck, K. Campanale, L. Hu, D.G. Hall, X.Y. Yang, M. Nakano, T.A. McNearney, J. Uetrecht, W. Landschulz, Dose-dependent acute liver injury with hypersensitivity features in humans due to a novel microsomal prostaglandin E synthase 1 inhibitor, Br. J. Clin. Pharmacol. 84 (2018) 179–188, doi:10.1111/bcp.13423.

[10] D. Xu, S.E. Rowland, P. Clark, A. Giroux, B. Côté, S. Guiral, M. Salem, Y. Ducharme, R.W. Friesen, N. Méthot, J. Mancini, L. Audoly, D. Riendeau, MF63 [2-(6-chloro-1H-phenanthro[9,10-*d*]imidazol-2-yl)-isophthalonitrile], a selective microsomal prostaglandin E synthase-1 inhibitor, relieves pyresis and pain in preclinical models of inflammation, J. Pharmacol. Exp. Ther. 326 (2008) 754–763, doi:10.1124/jpet.108.138776.use.

[11] T. Sjögren, J. Nord, M. Ek, P. Johansson, G. Liu, S. Geschwindner, Crystal structure of microsomal prostaglandin E2 synthase provides insight into diversity in the MAPEG superfamily, Proc. Natl. Acad. Sci. U.S.A. 110 (2013) 3806–3811, doi:10.1073/pnas.1218504110.

[12] L.R. Howe, K. Subbaramaiah, C.V. Kent, X.K. Zhou, S.H. Chang, T. Hla, P.J. Jakobsson, C.A. Hudis, A.J. Dannenberg, Genetic deletion of microsomal prostaglandin e synthase-1 suppresses mouse mammary tumor growth and angiogenesis, Prostaglandins Other Lipid Mediat 106 (2013) 99–105, doi:10.1016/j.prostaglandins.2013.04.002.

[13] R. Takahashi, H. Amano, T. Satoh, K. Tabata, M. Ikeda, H. Kitasato, S. Akira, M. Iwamura, M. Majima, Roles of microsomal prostaglandin E synthase-1 in lung metastasis formation in prostate cancer RM9 cells, Biomed. Pharmacother. 68 (2014) 71–77, doi:10.1016/j.biopha.2013.10.008.

[14] Y. Sasaki, Y. Nakatani, S. Hara, Role of microsomal prostaglandin E synthase-1 (mPGES-1)-derived prostaglandin E2 in colon carcinogenesis, Prostaglandins Other Lipid Mediat 121 (2015) 42–45, doi:10.1016/j.prostaglandins.2015.06.006.

[15] F. Finetti, E. Terzuoli, E. Bocci, I. Coletta, L. Polenzani, G. Mangano, M.A. Alisi, N. Cazzolla, A. Giachetti, M. Ziche, S. Donnini, Pharmacological inhibition of microsomal prostaglandin E synthase-1 suppresses epidermal growth factor receptor-mediated tumor growth and angiogenesis, PLoS ONE 7 (2012) e40576, doi:10.1371/journal.pone.0040576.

[16] Y. Zhu, M. Zhu, P. Lance, IL1B-mediated Stromal COX-2 signaling mediates proliferation and invasiveness of colonic epithelial cancer cells, Exp. Cell Res. 318 (2012) 2520–2530, doi:10.1016/j.yexcr.2012.07.021.

[17] D. Riendeau, R. Aspiotis, D. Ethier, Y. Gareau, E.L. Grimm, J. Guay, S. Guiral, H. Juteau, J.A. Mancini, N. Méthot, J. Rubin, R.W. Friesen, Inhibitors of the inducible microsomal prostaglandin E2 synthase (mPGES-1) derived from MK-886, Bioorg. Med. Chem. Lett. 15 (2005) 3352–3355, doi:10.1016/j.bmcl.2005.05.027.

[18] H.H. Chang, Z. Song, L. Wisner, T. Tripp, V. Gokhale, E.J. Meuillet, Identification of a novel class of anti-inflammatory compounds with anti-tumor activity in colorectal and lung cancers, Invest. New Drugs. 30 (2012) 1865–1877, doi:10.1007/s10637-011-9748-8.

[19] H. Hanaka, S.-C. Pawelzik, J.I. Johnsen, M. Rakonjac, K. Terawaki, A. Rasmuson, B. Sveinbjörnsson, M.C. Schumacher, M. Hamberg, B. Samuelsson, P.-J. Jakobsson, P. Kogner, O. Rådmark, Microsomal prostaglandin E synthase 1 determines tumor growth *in vivo* of prostate and lung cancer cells, Proc. Natl. Acad. Sci. U.S.A. 106 (2009) 18757–18762, doi:10.1073/pnas.0910218106.

[20] B.P. Van Rees, A. Sivula, S. Thorén, H. Yokozaki, P.J. Jakobsson, G.J.A. Offerhaus, A. Ristimäki, Expression of microsomal prostaglandin E synthase-1 in intestinal type gastric adenocarcinoma and in gastric cancer cell lines, Int. J. Cancer. 107 (2003) 551–556, doi:10.1002/ijc.11422.

[21] A. Kock, K. Larsson, F. Bergqvist, N. Eissler, L.H.M. Elfman, J. Raouf, M. Korotkova, J.I. Johnsen, P.J. Jakobsson, P. Kogner, Inhibition of Microsomal Prostaglandin E Synthase-1 in Cancer-Associated Fibroblasts Suppresses Neuroblastoma Tumor Growth, EBioMedicine 32 (2018) 84–92, doi:10.1016/j.ebiom.2018.05.008.

[22] H.N. Jabbour, S.A. Milne, A.R.W. Williams, R.A. Anderson, S.C. Boddy, Expression of COX-2 and PGE synthase and synthesis of PGE2 in endometrial adenocarcinoma: a possible autocrine/paracrine regulation of neoplastic cell function via EP2/EP4 receptors, Br. J. Cancer. 85 (2001) 1023–1031, doi:10.1038/sj.bjc.6692033.

[23] K. Yoshimatsu, D. Golijanin, P.B. Paty, C. Adenomas, R.A. Soslow, P. Jakobsson, R.A. Delellis, K. Subbaramaiah, Inducible microsomal prostaglandin E synthase is overexpressed in colorectal adenomas and cancer, Clin. Cancer Res. 7 (2001) 3971–3976 https://clincancerres.aacrjournals.org/content/7/12/3971.

[24] K. Yoshimatsu, N.K. Altorki, D. Golijanin, C.L. Cancer, F. Zhang, P. Jakobsson, A.J. Dannenberg, Inducible prostaglandin E synthase is overexpressed in non-small cell lung cancer, Clin. Cancer Res. 7 (2001) 2669–2674 https://pubmed.ncbi.nlm.nih.gov/11555578.

[25] H. Takeda, H. Miyoshi, Y. Tamai, M. Oshima, M.M. Taketo, Simultaneous expression of COX-2 and mPGES-1 in mouse gastrointestinal hamartomas, Br. J. Cancer. 90 (2004) 701–704, doi:10.1038/sj.bjc.6601584.

[26] Y. Li, S. Yin, D. Nie, S. Xie, L. Ma, X. Wang, Y. Wu, J. Xiao, MK886 inhibits the proliferation of HL-60 leukemia cells by suppressing the expression of mPGES-1 and reducing prostaglandin E2 synthesis, Int. J. Hematol. 94 (2011) 472–478, doi:10.1007/s12185-011-0954-0.

[27] X. Norel, Prostanoid receptors in the human vascular wall, Scientific World Journal 7 (2007) 1359–1374, doi:10.1100/tsw.2007.184.

[28] D. Wang, H. Wang, J. Brown, T. Daikoku, W. Ning, Q. Shi, A. Richmond, R. Strieter, S.K. Dey, R.N. DuBois, CXCL1 induced by prostaglandin E2 promotes angiogenesis in colorectal cancer, J. Exp. Med. 203 (2006) 941–951, doi:10.1084/jem.20052124.

[29] F.G. Buchanan, W. Chang, H. Sheng, J. Shao, J.D. Morrow, R.N. Dubois, Up-regulation of the enzymes involved in prostacyclin synthesis via Ras induces vascular endothelial growth factor, Gastroenterology 127 (2004) 1391–1400, doi:10.1053/j.gastro.2004.07.025.

[30] Y. Zhang, Y. Daaka, PGE2 promotes angiogenesis through EP4 and PKA Cγ pathway, Blood 118 (2011) 5355–5364, doi:10.1182/BLOOD-2011-04-350587.

[31] H. Amano, I. Hayashi, H. Endo, H. Kitasato, S. Yamashina, T. Maruyama, M. Kobayashi, K. Satoh, M. Narita, Y. Sugimoto, T. Murata, H. Yoshimura, S. Narumiya, M. Majima, Host prostaglandin E2-EP3 signaling regulates tumor-associated angiogenesis and tumor growth, J. Exp. Med. 197 (2003) 221–232, doi:10.1084/jem.20021408.

[32] H. Kamata, K. Hosono, T. Suzuki, Y. Ogawa, H. Kubo, H. Katoh, Y. Ito, S. Uematsu, S. Akira, M. Watanabe, M. Majima, MPGES-1-expressing bone marrow-derived cells enhance tumor growth and angiogenesis in mice, Biomed. Pharmacother. 64 (2010) 409–416, doi:10.1016/j.biopha.2010.01.017.

[33] D. Kamei, K. Yamakawa, Y. Takegoshi, M. Mikami-Nakanishi, Y. Nakatani, S. Oh-Ishi, H. Yasui, Y. Azuma, N. Hirasawa, K. Ohuchi, H. Kawaguchi, Y. Ishikawa, T. Ishii, S. Uematsu, S. Akira, M. Murakami, I. Kudo, Reduced pain hypersensitivity and inflammation in mice lacking microsomal prostaglandin E synthase-1, J. Biol. Chem. 279 (2004) 33684–33695, doi:10.1074/jbc.M400199200.

[34] D. Kamei, M. Murakami, Y. Sasaki, Y. Nakatani, M. Majima, Y. Ishikawa, T. Ishi, S. Uematsu, S. Akira, S. Hara, I. Kudo, Microsomal prostaglandin E synthase-1 in both cancer cells and hosts contributes to tumour growth, invasion and metastasis, Biochem. J. 425 (2010) 361–371, doi:10.1042/BJ20090045.

[35] M. De La Rosa, H.W. Kim, E. Gunic, C. Jenket, U. Boyle, Y. hyo Koh, I. Korboukh, M. Allan, W. Zhang, H. Chen, W. Xu, S. Nilar, N. Yao, R. Hamatake, S.A. Lang, Z. Hong, Z. Zhang, J.L. Girardet, Tri-substituted triazoles as potent non-nucleoside inhibitors of the HIV-1 reverse transcriptase, Bioorg. Med. Chem. Lett. 16 (2006) 4444–4449, doi:10.1016/j.bmcl.2006.06.048.

[36] P. Çikla-Süzgün, N. Kaushik-Basu, A. Basu, P. Arora, T.T. Talele, I. Durmaz, R. Çetin-Atalay, S.G. Küçükgüzel, Anti-cancer and anti-hepatitis C virus NS5B polymerase activity of etodolac 1,2,4-triazoles, J. Enzyme Inhib. Med. Chem. 30 (2015) 778–785, doi:10.3109/14756366.2014.971780.

[37] İ. Küçükgüzel, Ş.G. Küçükgüzel, S. Rollas, M. Kiraz, Some 3-thioxo/alkylthio-1,2,4-triazoles with a substituted thiourea moiety as possible antimycobacterials, Bioorg. Med. Chem. Lett. 11 (2001) 1703–1707, doi:10.1016/S0960-894X(01)00283-9.

[38] İ. Küçükgüzel, E. Tatar, Ş.G. Küçükgüzel, S. Rollas, E. De Clercq, Synthesis of Some Novel Thiourea Derivatives Obtained from 5-[(4-Aminophenoxy)methyl]-4-alkyl/aryl-2,4-dihydro-3H-1,2,4-triazole-3-thiones and Evaluation as Antiviral/anti-HIV and Antituberculosis Agents, Eur. J. Med. Chem. 43 (2008) 381–392, doi:10.1002/chin.200829219.

[39] N.N. Gülerman, H.N. Doğan, S. Rollas, C. Johansson, C. Çelik, Synthesis and structure elucidation of some new thioether derivatives of 1, 2, 4-triazoline-3-thiones and their antimicrobial activities, Farmaco 56 (2001) 953–958, doi:10.1016/s0014-827x(01)01167-3.

[40] M. Amir, K. Shikha, Synthesis and anti-inflammatory, analgesic, ulcerogenic and lipid peroxidation activities of some new 2-[(2,6-dichloroanilino) phenyl]acetic acid derivatives, Eur. J. Med. Chem. 39 (2004) 535–545, doi:10.1016/j.ejmech.2004.02.008.

[41] E. Palaska, G. Şahin, P. Kelicen, N.T. Durlu, G. Altinok, Synthesis and anti-inflammatory activity of 1-acylthiosemicarbazides, 1,3,4-oxadiazoles, 1,3,4-thiadiazoles and 1,2,4-triazole-3-thiones, Farmaco 57 (2002) 101–107, doi:10.1016/S0014-827X(01)01176-4.

[42] U. Salgin-Gökşen, N. Gökhan-Kelekçi, Ö. Göktaş, Y. Köysal, E. Kiliç, Ş. Işik, G. Aktay, M. Özalp, 1-Acylthiosemicarbazides, 1,2,4-triazole-5(4H)-thiones, 1,3,4-thiadiazoles and hydrazones containing 5-methyl-2-benzoxazolinones: synthesis, analgesic-anti-inflammatory and antimicrobial activities, Bioorg. Med. Chem. 15 (2007) 5738–5751, doi:10.1016/j.bmc.2007.06.006.

[43] Ş.G. Küçükgüzel, I. Küçükgüzel, E. Tatar, S. Rollas, F. Şahin, M. Güllüce, E. De Clercq, L. Kabasakal, Synthesis of some novel heterocyclic compounds derived from diflunisal hydrazide as potential anti-infective and anti-inflammatory agents, Eur. J. Med. Chem. 42 (2007) 893–901, doi:10.1016/j.ejmech.2006.12.038.

[44] A.T. Mavrova, D. Wesselinova, Y.A. Tsenov, P. Denkova, Synthesis, cytotoxicity and effects of some 1,2,4-triazole and 1,3,4-thiadiazole derivatives on immunocompetent cells, Eur. J. Med. Chem. 44 (2009) 63–69, doi:10.1016/j.ejmech.2008.03.006.
[45] W.A. El-Sayed, E.M. Flefel, E.M.H. Morsy, Anticancer and antimicrobial activities of some synthesized pyrazole and triazole derivatives, Der Pharma Chem 4 (2012) 23–32.
[46] T. Singha, J. Singh, A. Naskar, T. Ghosh, A. Monda, M. Kundu, R.K. Harwansh, T.K. Maity, Synthesis and evaluation of antiproliferative activity of 1,2,4-triazole derivatives against EAC bearing mice model, Indian J. Pharm. Educ. Res. 46 (2012) 346–351, doi:10.5530/ijper.47.4.7.
[47] N. Kulabaş, E. Tatar, O. Bingol Özakpınar, D. Özsavcı, C. Pannecouque, E. De Clercq, İ. Küçükgüzel, Synthesis and antiproliferative evaluation of novel 2-(4H-1,2,4-triazole-3-ylthio)acetamide derivatives as inducers of apoptosis in cancer cells, Eur. J. Med. Chem. 121 (2016) 58–70, doi:10.1016/j.ejmech.2016.05.017.
[48] I. Khan, S. Ali, S. Hameed, N.H. Rama, M.T. Hussain, A. Wadood, R. Uddin, Z. Ul-Haq, A. Khan, S. Ali, M.I. Choudhary, Synthesis, antioxidant activities and urease inhibition of some new 1,2,4-triazole and 1,3,4-thiadiazole derivatives, Eur. J. Med. Chem. 45 (2010) 5200–5207, doi:10.1016/j.ejmech.2010.08.034.
[49] M.S. Karthikeyan, D.J. Prasad, B. Poojary, K. Subrahmanya Bhat, B.S. Holla, N.S. Kumari, Synthesis and biological activity of Schiff and Mannich bases bearing 2,4-dichloro-5-fluorophenyl moiety, Bioorg. Med. Chem. 14 (2006) 7482–7489, doi:10.1016/j.bmc.2006.07.015.
[50] I.R. Ezabadi, C. Camoutsis, P. Zoumpoulakis, A. Geronikaki, M. Soković, J. Glamočilija, A. Ćirić, Sulfonamide-1,2,4-triazole derivatives as antifungal and antibacterial agents: synthesis, biological evaluation, lipophilicity, and conformational studies, Bioorg. Med. Chem. 16 (2008) 1150–1161, doi:10.1016/j.bmc.2007.10.082.
[51] T. Önkol, D. Doğruer, L. Uzun, S. Adak, S. Özkan, M.F. Sahin, Synthesis and antimicrobial activity of new 1,2,4-triazole and 1,3,4-thiadiazole derivatives, J. Enzyme Inhib. Med. Chem. 23 (2008) 277–284, doi:10.1080/14756360701408697.
[52] H.A. Saadeh, I.M. Mosleh, A.G. Al-Bakri, M.S. Mubarak, Synthesis and antimicrobial activity of new 1,2,4-triazole-3-thiol metronidazole derivatives, Monatsh. Chem. 141 (2010) 471–478, doi:10.1007/s00706-010-0281-9.
[53] F.H. Havaldar, A.R. Patil, Syntheses of 1, 2, 4 triazole derivatives and their biological activity, E-Journal Chem 5 (2008) 347–354, doi:10.1155/2008/394737.
[54] S. He, C. Li, Y. Liu, L. Lai, Discovery of Highly Potent Microsomal Prostaglandin E 2 Synthase 1 Inhibitors Using the Active Conformation Structural Model and Virtual Screen, J. Med. Chem. 56 (2013) 3296–3309, doi:10.1021/jm301900x.
[55] G. Erensoy, K. Ding, C.G. Zhan, A. Elmezayen, K. Yelekçi, M. Duracik, Ö. Bingöl Özakpinar, İ. Küçükgüzel, Synthesis, in silico studies and cytotoxicity evaluation of novel 1,3,4-oxadiazole derivatives designed as potential mPGES-1 inhibitors, J. Res. Pharm. 24 (2020) 436–451, doi:10.35333/jrp.2020.187.
[56] S.D. Bagul, J.D. Rajput, M.M. Patil, R.S. Bendre, Synthesis, characterization and antioxidant activity of carvacrol based sulfonates, Med. Chem. (Los Angeles) 7 (2017) 294–298, doi:10.4172/2161-0444.1000470.
[57] M. Abdel-Aziz, G.E.D.A.A. Abou-Rahma, E.A.M. Beshr, T.F.S. Ali, New nitric oxide donating 1,2,4-triazole/oxime hybrids:synthesis, investigation of anti-inflammatory, ulceroginic liability and anti-proliferative activities, Bioorg. Med. Chem. 21 (2013) 3839–3849, doi:10.1016/j.bmc.2013.04.022.
[58] A. Hamza, M. Tong, M.D.M. Abdulhameed, J. Liu, A.C. Goren, H.H. Tai, C.G. Zhan, Understanding microscopic binding of human microsomal prostaglandin e synthase-1 (mPGES-1) trimer with substrate PGH2 and cofactor GSH: insights from computational alanine scanning and site-directed mutagenesis, J. Phys. Chem. B. 114 (2010) 5605–5616, doi:10.1021/jp100668y.
[59] K. Ding, Z. Zhou, S. Hou, Y. Yuan, S. Zhou, X. Zheng, J. Chen, C. Loftin, F. Zheng, C.G. Zhan, Structure-based discovery of mPGES-1 inhibitors suitable for preclinical testing in wild-type mice as a new generation of anti-inflammatory drugs, Sci. Rep. 8 (2018) e5205, doi:10.1038/s41598-018-23482-4.
[60] K. Ding, Z. Zhou, S. Zhou, Y. Yuan, K. Kim, T. Zhang, X. Zheng, F. Zheng, C.G. Zhan, Design, synthesis, and discovery of 5-((1,3-diphenyl-1H-pyrazol-4-yl)methylene)pyrimidine-2,4,6(1H,3H,5H)-triones and related derivatives as novel inhibitors of mPGES-1, Bioorg. Med. Chem. Lett. 28 (2018) 858–862, doi:10.1016/j.bmcl.2018.02.011.
[61] A. Hamza, X. Zhao, M. Tong, H.H. Tai, C.G. Zhan, Novel human mPGES-1 inhibitors identified through structure-based virtual screening, Bioorg. Med. Chem. 19 (2011) 6077–6086, doi:10.1016/j.bmc.2011.08.040.
[62] Z. Zhou, Y. Yuan, S. Zhou, K. Ding, F. Zheng, C.G. Zhan, Selective inhibitors of human mPGES-1 from structure-based computational screening, Bioorg. Med. Chem. Lett. 27 (2017) 3739–3743, doi:10.1016/j.bmcl.2017.06.075.
[63] L. Harding, Z. Wang, H. Tai, Stimulation of prostaglandin E 2 synthesis by interleukin-1/3 is amplified by interferons but inhibited by interleukin-4 in human amnion-derived WISH cells, Biochim. Biophys. Acta. 1310 (1996) 48–52.
[64] G.M. Morris, R. Huey, W. Lindsrom, M.F. Sanner, R.K. Belew, D.S. Goodsell, A.J. Olson, AutoDock4 and AutoDockTools4: automated docking with selective receptor flexibility, J. Comput. Chem. 30 (2009) 2785–2791, doi:10.1002/jcc.21256.
[65] S.L. Kuklish, S. Antonysamy, S.N. Bhattachar, S. Chandrasekhar, M.J. Fisher, A.J. Fretland, K. Gooding, A. Harvey, N.E. Hughes, J.G. Luz, P.R. Manninen, J.E. McGee, A. Navarro, B.H. Norman, K.M. Partridge, S.J. Quimby, M.A. Schiffler, A.V. Sloan, A.M. Warshawsky, J.S. York, X.P. Yu, Characterization of 3,3-dimethyl substituted N-aryl piperidines as potent microsomal prostaglandin E synthase-1 inhibitors, Bioorg. Med. Chem. Lett. 26 (2016) 4824–4828, doi:10.1016/j.bmcl.2016.08.023.
[66] K.C. Duggan, M.J. Walters, J. Musee, J.M. Harp, J.R. Kiefer, J.A. Oates, L.J. Marnett, Molecular basis for cyclooxygenase inhibition by the non-steroidal anti-inflammatory drug naproxen, J. Biol. Chem. 285 (2010) 34950–34959, doi:10.1074/jbc.M110.162982.
[67] G.M. Morris, D.S. Goodsell, R.S. Halliday, R. Huey, W.E. Hart, R.K. Belew, A.J. Olson, Automated docking using a Lamarckian genetic algorithm and an empirical binding free energy function, J. Comput. Chem. 19 (1998) 1639–1662 10.1002/(SICI)1096-987X(19981115)19:14≤1639::AIDJCC10≥3.0.CO;2-B.
[68] J.C. Phillips, R. Braun, W. Wang, J. Gumbart, E. Tajkhorshid, E. Villa, C. Chipot, R.D. Skeel, L. Kalé, K. Schulten, Scalable molecular dynamics with NAMD, J. Comput. Chem. 26 (2005) 1781–1802, doi:10.1002/jcc.20289.
[69] A.L. Lomize, I.D. Pogozheva, M.A. Lomize, H.I. Mosberg, Positioning of proteins in membranes: a computational approach, Protein Sci 15 (2006) 1318–1333, doi:10.1110/ps.062126106.
[70] J. Lee, X. Cheng, J.M. Swails, M.S. Yeom, P.K. Eastman, J.A. Lemkul, S. Wei, J. Buckner, J.C. Jeong, Y. Qi, S. Jo, V.S. Pande, D.A. Case, C.L. Brooks, A.D. MacKerell, J.B. Klauda, W. Im, CHARMM-GUI input generator for NAMD, GROMACS, AMBER, OpenMM, and CHARMM/OpenMM simulations using the CHARMM36 additive force field, J. Chem. Theory Comput. 12 (2016) 405–413, doi:10.1021/acs.jctc.5b00935.
[71] A. Daina, O. Michielin, V. Zoete, SwissADME: a free web tool to evaluate pharmacokinetics, drug-likeness and medicinal chemistry friendliness of small molecules, Sci. Rep. 7 (2017) 1–13, doi:10.1038/srep42717.
[72] D.E.V. Pires, T.L. Blundell, D.B. Ascher, pkCSM: predicting small-molecule pharmacokinetic and toxicity properties using graph-based signatures, J. Med. Chem. 58 (2015) 4066–4072, doi:10.1021/acs.jmedchem.5b00104.
[73] T. Sander, J. Freyss, M. Von Korff, C. Rufener, DataWarrior: an open-source program for chemistry aware data visualization and analysis, J. Chem. Inf. Model. 55 (2015) 460–473, doi:10.1021/ci500588j.
[74] M. Koparir, A. Çetin, A. Cansiz, 5-Furan-2yl[1,3,4]oxadiazole-2-thiol, 5-furan-2yl-4h [1,2,4] triazole-3-thiol and their thiol-thione tautomerism, Molecules 10 (2005) 475–480, doi:10.3390/10020475.
[75] G. Lacesse, J.M. Muchowski, Five-membered Heterocyclic Thiones. Part II, Oxazole-2-thione 50 (1972) 3082–3083.
[76] M.S. Behalo, M.S. Amine, I.M. Fouda, Regioselective synthesis, antitumor and antioxidant activities of some 1,2,4-triazole derivatives based on 4-phenyl-5-(quinolin-8-yloxy)methyl-4H-1,2,4-triazole-3-thiol, Phosphorus, Sulfur Silicon Relat. Elem. 192 (2017) 410–417, doi:10.1080/10426507.2016.1247087.
[77] S. Namkoong, S.J. Lee, C.K. Kim, Y.M. Kim, H.T. Chung, H. Lee, J.A. Han, K.S. Ha, Y.G. Kwon, Y.M. Kim, Prostaglandin E2 stimulates angiogenesis by activating the nitric oxide/cGMP pathway in human umbilical vein endothelial cells, Exp. Mol. Med. 37 (2005) 588–600, doi:10.1038/emm.2005.72.
[78] L. Zhao, Y. Wu, Z. Xu, H. Wang, Z. Zhao, Y. Li, P. Yang, X. Wei, Involvement of COX-2/PGE2 signalling in hypoxia-induced angiogenic response in endothelial cells, J. Cell. Mol. Med. 16 (2012) 1840–1855, doi:10.1111/j.1582-4934.2011.01479.x.
[79] Y. Kubota, H.K. Kleinman, G.R. Martin, T.J. Lawley, Role of laminin and basement membrane in the morphological differentiation of human endothelial cells into capillary-like structures, J. Cell Biol. 107 (1988) 1589–1598, doi:10.1083/jcb.107.4.1589.
[80] M.D. Salvado, A. Alfranca, J.Z. Haeggström, J.M. Redondo, Prostanoids in tumor angiogenesis: therapeutic intervention beyond COX-2, Trends Mol. Med. 18 (2012) 233–243, doi:10.1016/j.molmed.2012.02.002.
[81] P. Khurana, S.M. Jachak, Chemistry and biology of microsomal prostaglandin E2 synthase-1 (mPGES-1) inhibitors as novel anti-inflammatory agents: recent developments and current status, RSC Adv 6 (2016) 28343–28369, doi:10.1039/c5ra25186a.
[82] Y.H. Zhao, M.H. Abraham, J. Le, A. Hersey, C.N. Luscombe, G. Beck, B. Sherborne, I. Cooper, Rate-limited steps of human oral absorption and QSAR studies, Pharm. Res. 19 (2002) 1446–1457, doi:10.1023/A:1020444330011.
[83] M.F. Froom, P-glycoprotein: a defense mechanism limiting oral bioavailability and CNS accumulation of drugs, J. Clin. Pharmacol. Ther. 38 (2000) 69–74.
[84] R.B. van Breemen, Y. Li, Caco-2 cell permeability assays to measure drug absorption, Expert Opin. Drug Metab. Toxicol. 1 (2005) 175–185.
[85] J.B. Baell, G.A. Holloway, New substructure filters for removal of pan assay interference compounds (PAINS) from screening libraries and for their exclusion in bioassays, J. Med. Chem. 53 (2010) 2719–2740, doi:10.1021/jm901137j.
[86] R. Brenk, A. Schipani, D. James, A. Krasowski, I.H. Gilbert, J. Frearson, P.G. Wyatt, Lessons learnt from assembling screening libraries for drug discovery for neglected diseases, ChemMedChem 3 (2008) 435–444, doi:10.1002/cmdc.200700139.